

Review

Cell-Surface Glycan Labeling and Sensing

Yiran Li ¹ , Lele Wang ¹, Lin Ding ^{1,2,*}  and Huangxian Ju ¹

¹ State Key Laboratory of Analytical Chemistry for Life Science, School of Chemistry and Chemical Engineering, Nanjing University, Nanjing 210023, China; liyiranfighting@126.com (Y.L.); llwang1620@163.com (L.W.); hxju@nju.edu.cn (H.J.)

² Chemistry and Biomedicine Innovation Center (ChemBIC), Nanjing University, Nanjing 210023, China

* Correspondence: dinglin@nju.edu.cn

Abstract: Cell-surface glycans are abundant and complex and play a critical role in maintaining protein stability, regulating cell behavior, and participating in cell communication. Obtaining structural information on glycans in situ is helpful to further understand the role of glycans in the physiological and pathological processes of cells and the regulatory mechanism. To achieve this, we can use recognition or labeling strategies to convert the presence of glycans on the cell surface into signals that can be detected. Currently, many different types of in situ sensing strategies for glycans have been developed. The spatial control of the conversion process can realize the restriction of glycan detection to specific proteins, and the introduction of signal amplification technology into the conversion process can improve the sensitivity of sensing. In this paper, the recent progress of glycan labeling methods and sensing technology is reviewed, and the future development direction is prospected.

Keywords: cell surface; glycan imaging; glycan labeling; glycan sensing; live cells

1. Introduction

Carbohydrates are the main source of energy required by all living organisms to sustain life activities. They also act as structural and functional components by modifying proteins or lipids to form glycoproteins or glycolipids. The carbohydrate portion of these conjugates is called glycans, which are composed of a variety of monosaccharides linked in different orders. In mammals, for example, 50% of proteins are glycoproteins, and the glycan chains are made up of 17 types of monosaccharides [1]. The glycan chains can be attached to a nitrogen atom of Asn residues at Asn-X-Ser/Thr motifs (known as N-glycans) or to an oxygen atom of Ser or Thr residues (known as O-glycans) [2].

During physiological and pathological processes, the composition and structure of cell-surface glycans are changing dynamically. The alteration of glycan chains is strongly associated with immune disorders, microbial infection, tumor development [2,3], etc. Immunoglobulins and most complements in humoral immunity are glycosylated [3]. Glycosylation not only increases protein stability but is also involved in recognition events in the body. In rheumatoid arthritis (an autoimmune disease), the absence of galactosylated immunoglobulin G leads to the aggregation of the mannose-binding lectin and results in pathology [4,5]. At the classical interface of microbial–host interactions, the apical part of the intestinal epithelium is enriched with glycan components, especially α 1,2-fucose [6]. *Candida albicans* can infect α 1,2-fucose-deficient intestines. There is also increasing evidence that glycosylation plays a role in tumorigenesis and metastasis [2,7]. Alterations in cell-surface glycosylation, particularly terminal glycans, can promote the invasive behavior of tumor cells and ultimately lead to cancer progression.

As a promising biomarker, glycans have important research significance and broad application prospects in disease diagnosis and treatment. The development of glycan labeling methods and the establishment of specific sensing strategies will help to obtain spatio-temporal glycan expression information, which is crucial for understanding the



Citation: Li, Y.; Wang, L.; Ding, L.; Ju, H. Cell-Surface Glycan Labeling and Sensing. *Targets* **2024**, *2*, 1–31. <https://doi.org/10.3390/targets2010001>

Academic Editor: Bruno Rizzuti

Received: 4 November 2023

Revised: 24 December 2023

Accepted: 29 December 2023

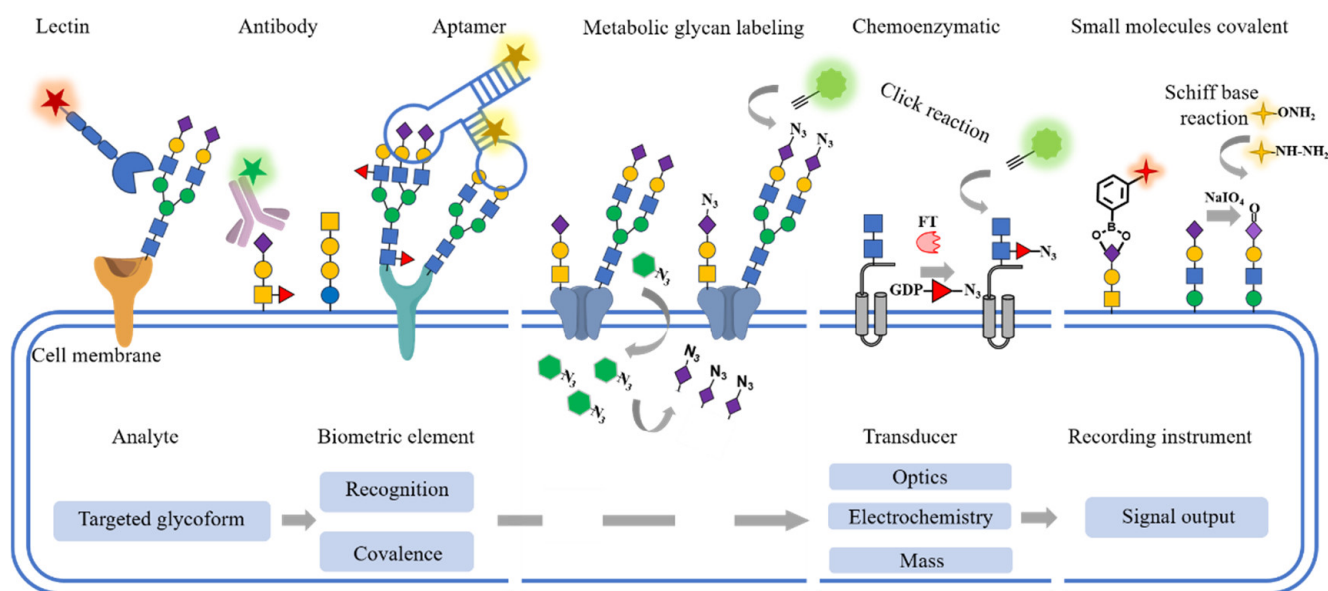
Published: 31 December 2023



Copyright: © 2023 by the authors. Licensee MDPI, Basel, Switzerland. This article is an open access article distributed under the terms and conditions of the Creative Commons Attribution (CC BY) license (<https://creativecommons.org/licenses/by/4.0/>).

regulatory mechanisms and biological effects of glycans on cell surfaces. Using the glycan sensing strategies, it is possible to understand the changing characteristics of glycans during the onset and development of diseases and provide new biomarkers and diagnostic methods for early diagnosis of diseases [8–10]. At the same time, in the field of disease treatment, glycan detection methods can also provide technical support and model validation methods for drug development [11–14], which is conducive to the expansion and innovation of therapeutic strategies.

The in situ sensing of glycans on cell membrane surfaces presents several challenges: (1) carbohydrate isomers are diverse and difficult to distinguish; (2) glycosylation is a non-template synthesis process with microscopic inhomogeneity of modification sites; and (3) glycoconjugates on the surface of cell membranes are functionally complex and low in abundance. To establish methods for in situ glycan analysis, the development of various labeling or recognition strategies with superior specificity is a prerequisite. Achieving glycan analysis results with enhanced sensitivity and reduced detection limits requires the design of signal amplification strategies in glycan sensing. This review introduces natural and artificial molecules that recognize glycans on the cell surface, outlines the different labeling strategies for glycan structures, and focuses on specific glycan sensing strategies to quantify different glycoconjugates on cell membranes (Scheme 1).



Scheme 1. Schematic of various glycan labeling strategies and the integration of sensing elements for cell-surface glycan detection.

2. Glycan Recognition

The specific recognition and stable binding of glycans is an important basis for the identification and detection of glycans. Common glycan recognition molecules include lectins, aptamers, and antibodies (Table 1). Based on these molecules, various strategies for glycan analysis and monitoring have been developed, especially in situ glycan analysis methods.

2.1. Lectins

Lectins, a group of proteins produced by animal and plant cells, exhibit specific saccharide-binding abilities without invoking an immune response [15–17]. Researchers usually use lectins to isolate and purify glycoproteins [18,19], to identify glycoforms [20–26], or to regulate the differentiation [27] and maturation [28] of cells, etc. The affinity of lectins towards glycans is generally in the micromolar range due to the shallow binding pocket on the lectin surface exposed to competing solvent interactions [29]. However, in biological environments, some lectins can assemble into homopolymeric structures with multiple binding sites to achieve superior affinity and selectivity. Thus, an oligomer can interact

efficiently with different arms of a branched oligosaccharide or with different glycan motifs of the same glycoprotein. In such an oligomeric arrangement, a high degree of multivalency can be achieved, driving affinity to the nanomolar range. For the investigation of lectin recognition of glycans, Beckwith et al. utilized an isothermal titration calorimetry (ITC) strategy to study the mechanisms underlying the interaction between human macrophage galactose-type lectin (hMGL) and mucin 1 (MUC1) synthetic peptides containing Tn antigen. They evaluated the impact of glycan site and glycosylation frequency on lectin recognition and revealed that the lifetime of lectin–glycan complexes extends with an increase in glycan valency [30].

To track the lectin binding events, Li et al. covalently coupled fluorescent molecules to lectins using a “ligand-directed labeling” method [31], and the prepared fluorescently labeled *Ricinus Communis* Agglutinin I (RCA₁₂₀) and Sialic acid-binding Ig-like lectin 2-Fc (Siglec-2-Fc) were used for the detection of glycoproteins on HeLa cells (Figure 1). Lectin recognition can also be used to mediate proximity-covalent labeling. Xie et al. used lectin-proximal oxidative labeling (Lectin PROXL) to identify cell-surface glycoproteins bearing glycans recognized by lectins [32]. This approach provides an unprecedented view of lectin interactions with specific glycoproteins and protein networks mediated via specific glycans on cell membranes.

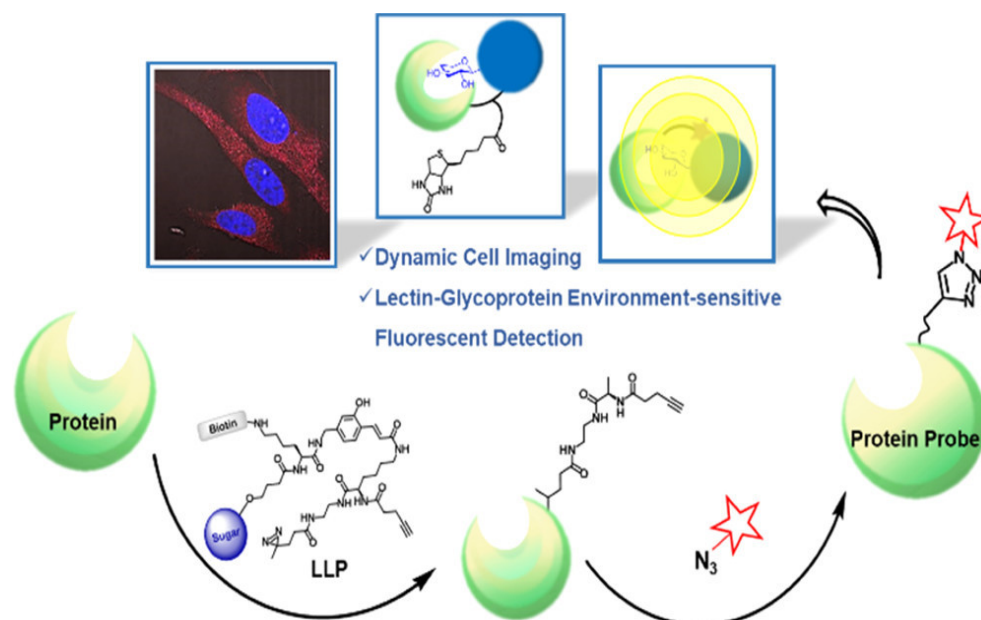


Figure 1. Schematic of lectin modification using “ligand-directed labeling probe (LLP)” method for lectin–glycoprotein interaction imaging [31]. Reproduced with permission from 31; published by the American Chemical Society, 2020.

2.2. Antibodies

Antibodies are protein molecules generated by immune responses that are capable of binding to specific epitopes on corresponding antigens. Antibodies exhibit superior affinity and selectivity for glycans when compared to lectins. However, obtaining anti-glycan antibodies is challenging due to the abundance of polysaccharides expressed on cell surfaces and their limited immunogenicity. Wang et al. utilized bacteriophage Q β conjugated with representative N-glycans to achieve immunogenicity [33]. And they discovered that the N-glycan-Q β immunogens connected with adipic acid linkers produced higher levels of glycan-specific antibodies than the N-glycan-triazole-Q β immunogens. Recognition of polysaccharide structures has led to the development of several antibodies. For example, carbohydrate antigen 19-9 (CA19-9), also known as the sialylated Lewis antigen (sLe^a), is a typical tumor marker characterized by a tetrasaccharide structure. Since the first antibody, 1116NS-19, against CA19-9 was obtained in 1979 [34,35], several high-affinity

antibodies for the specific recognition of the glycan structure have been developed and have found extensive application in the early diagnosis of cancer, especially pancreatic cancer [36,37]. The Lewis x's antibody anti-SSEA-1 is the most studied glycan antibody, which has been used to image inflammatory diseases [38] or to study the effect of altering the chemical structure of the glycans on anti-SSEA-1 binding [39]. This type of antibody possesses the ability to specifically resolve glycans, both to quantify the abundance of related glycoforms and to affect the function of related glycoforms by exhibiting a blocking effect. While there are other antibodies against classical glycan antigens, such as anti-Thomsen–Friedenreich glycoantigen (TF) [40], anti- α -Gal [41], anti-Gal- α 1,3-Gal (Galili antigen) [42], anti-GalNAc- α 1,3-GalNAc (Forssman antigen) [43], etc., their application in *in situ* cellular glycan analysis has yet to be thoroughly investigated.

2.3. Aptamers

In vitro SELEX-derived aptamers, including single-stranded DNA or RNA oligonucleotides, exhibit affinities comparable to, or even superior to, antibodies. Aptamers are cost-effective and readily available, offering a wide range of recognition capabilities spanning from small molecules to entire cells, thus having extensive potential applications [44,45]. In the field of glycan recognition, researchers have made considerable efforts to increase the affinities by improving the screening strategies, although sometimes the application environment of the aptamer is different from the screening environment, which hampers the affinity to some extent. The aptamers for three monosaccharides, galactose, glucose, and mannose, were screened *in vitro* by Sugimoto's laboratory in 1998 [46]. However, the affinity for galactose is only 10^{-4} ~ 10^{-5} M, which is not sufficient for *in situ* cellular recognition. Masud et al. proposed a novel cationic-charged modified DNA aptamer obtained using the magnetic particle-based SELEX method [47]. The K_d for the aptamer with the highest affinity to sialyllactose (SL-11) was 4.9 μ M. Zhou's group screened an ssDNA aptamer for sialyllactose with an affinity of 152.3 nM using magnetic separation-based SELEX and post-SELEX truncation methods [48].

Jeong and coworkers generated an RNA aptamer against sialyl Lewis X (sLe^x) [49] with K_d around 10^{-9} to 10^{-11} M. However, the aptamer shows a relatively low affinity for other neutral sugars (around 10^{-5} to 10^{-7} M). In addition to the simple screening of glycan-specific aptamers, Ma et al. developed a glycan-imprinted magnetic nanoparticle (MNP)-based SELEX method to efficiently screen aptamers against glycoproteins [50]. This strategy provides a new tool for screening glycan aptamers and enables the acquisition of glycoprotein-binding aptamers with a K_d of less than 1 nM.

Despite some progress in glycan-related aptamer screening, most screening methods are still based on some classical glycoprotein structures, such as RNase B, MUC1, etc. Screening for aptamers against glycopeptides using molecular imprinting is a promising approach [51]. Since glycan synthesis is not template-dependent, the same glycoprotein/glycolipid may have different glycosylation modifications in different cells, which may hamper the application of aptamers. Therefore, the development of screening techniques for aptamers targeting different glycoforms will help us better discriminate glycans in living systems.

3. Glycan Covalent Labeling

In addition to the recognition-based glycan labeling strategies mentioned above, covalent glycan labeling methods are also widely used and can be coupled to a variety of detection techniques, which include metabolic glycan labeling, chemoenzymatic glycan labeling (CeGL), and chemical covalent labeling (Table 2).

3.1. Metabolic Glycan Labeling (MGL)

MGL is a strategy for introducing bioorthogonal reporters into glycosylation sites. Unnatural monosaccharide substrates containing chemically reactive groups were linked to glycan or polypeptide chains, followed by bioorthogonal reactions for cell-surface labeling

and detection [52,53]. The key to this technique, which dates back to the 1970s [54–56], is the selection of unnatural reactive groups that can be stably modified into monosaccharide substrates without interfering with their recognition using glycan biosynthetic enzymes. To date, azide and alkyne groups have been the most widely used [57,58], both of which are inert in biological systems, cause little structural perturbation to monosaccharide substrates, and can be used as bioorthogonal chemical reporters.

MGL has a wide range of applications in glycan-related research, such as quantitative glycan analysis, glycomics, and glycofunctional studies. Chen and co-workers metabolically labeled the glycans on cancer cells *in vivo* and employed ^{19}F labeling to achieve selective cellular MRI imaging [59]. Wang and co-workers metabolically incorporated unnatural *N*-acetylhexosamine analogs (Figure 2) into the capsule polysaccharides of *Escherichia coli* and *Bacillus subtilis* via bacterial metabolism [60]. The site-specific introduction of fluorophores directly onto cell surfaces provides a method for observing and quantifying bacteria.

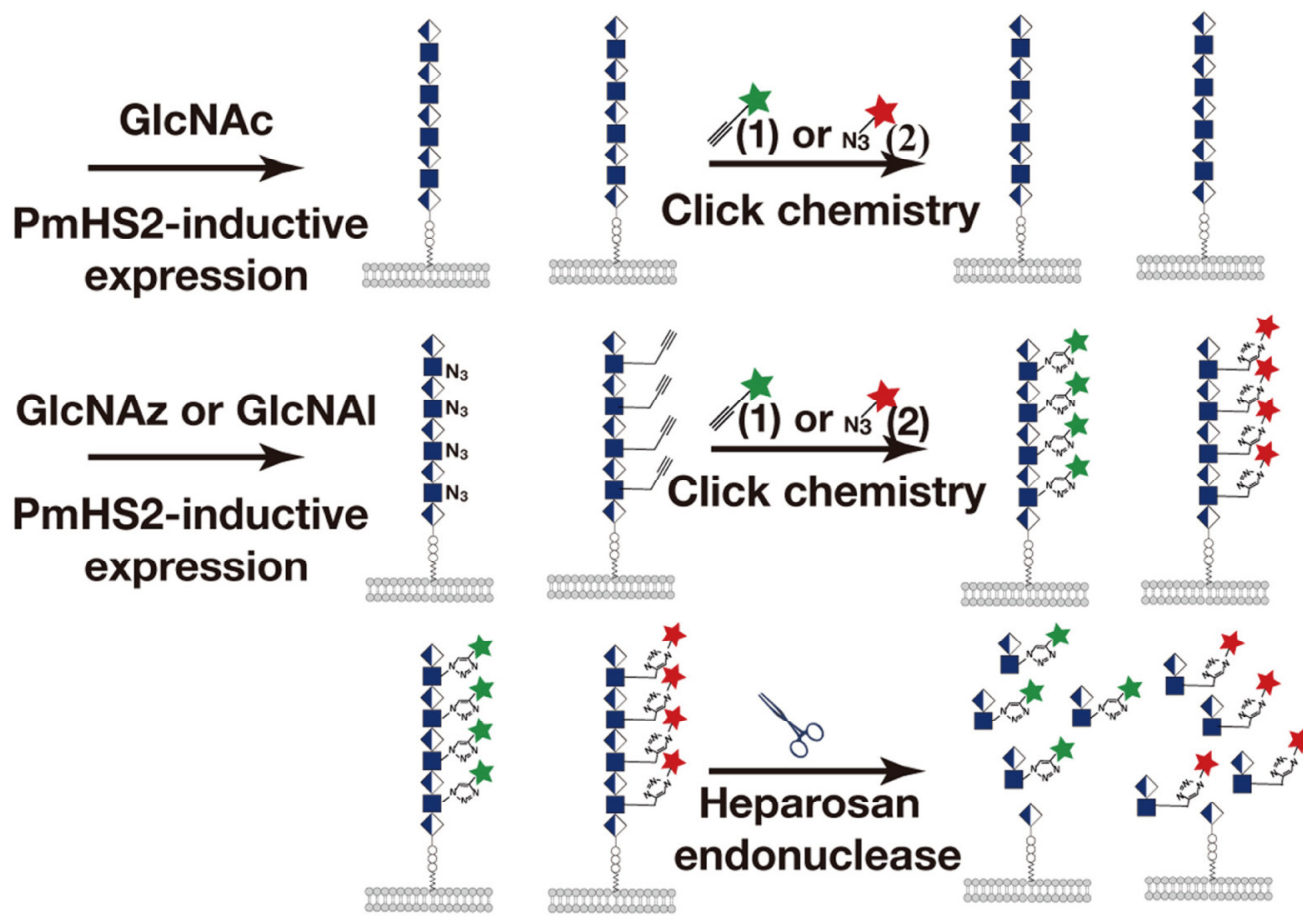


Figure 2. GlcNAc analogs are incorporated into the disaccharide repeat units of the cell-surface capsular polysaccharide *E. coli* K5. Both *N*-azidoacetyl-D-glucosamine (GlcNAz)- and *N*-pentynylacetylglucosamine (GlcNAI)-supplemented K5 were able to react with fluorescein amidite (FAM)-alkyne (1) or rhodamine- N_3 chloride (2) [60]. Reproduced with permission from 60 published by Science, 2023.

In addition to the advances in applications, metabolic monomers of unnatural sugars are also being developed at a rapid pace. Parle and co-workers sought to vary the extent of acetylation of methylcyclopropene (Cyoc)-tagged monosaccharides and investigate its effect on the extent of glycan labeling in various cancer cell lines [61]. They found that tri- and diacetylated derivatives significantly enhanced cell labeling compared to the tetra-acetylated monosaccharide. Chen's group found that per-*O*-acetylated unnatural monosaccharides can react non-specifically with protein cysteines via a non-enzymatic reac-

tion termed S-glyco-modification [62,63], and they synthesized unnatural monosaccharides including ManNAz, 1,3-Pr₂ManNAz, and 1,6-Pr₂ManNAz (Figure 3), which can avoid S-glyco-modification and allow for imaging of sialylated glycans [64]. The future direction of MGL development may lie in avoiding metabolic by-products, conferring selectivity or targeting, and creating novel unnatural sugar molecules.

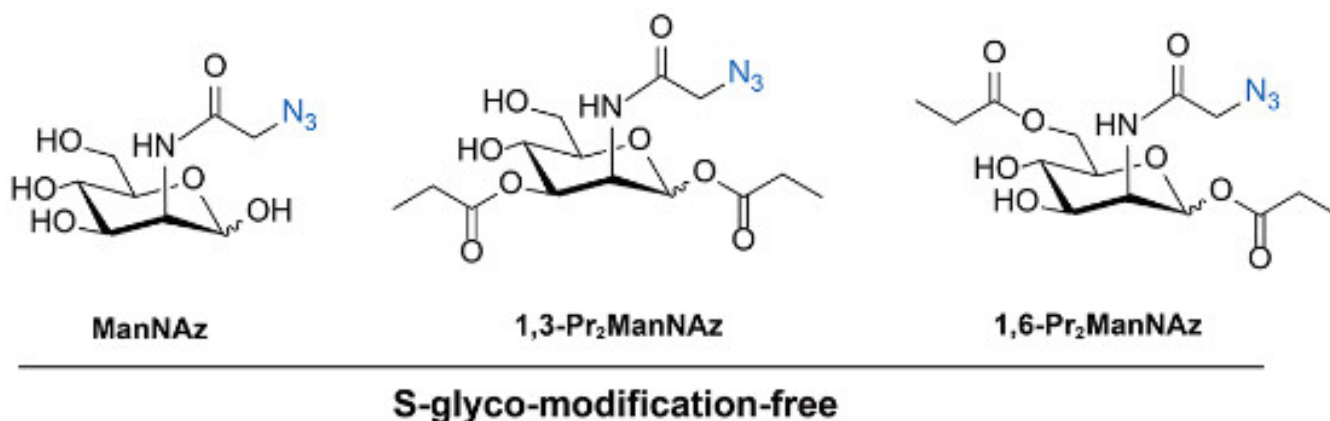


Figure 3. Structures of S-glyco-modification-free metabolic sugars [64]. Reproduced with permission from 64; published by the American Chemical Society, 2023.

3.2. Chemoenzymatic Glycan Labeling (CeGL)

Besides metabolic labeling, chemoenzyme labeling is one of the most important tools for covalent labeling of glycans. This technique simplifies the labeling process by transferring the functionalized unnatural monosaccharide or higher-order-structure sugar substrate directly to the end of the glycan chain, catalyzed via glycosyltransferases, and then labeling the signal probe through bioorthogonal reactions. These glycosyltransferases are highly specific and efficient catalysts capable of transferring monosaccharide substrates in a short time and are independent of the cellular biosynthetic process, allowing them to be used in any biological system that cannot be cultured with non-natural sugar analogs, such as human tissue extracts.

Wu's group summarized the available methods for chemoenzymatic labeling of glycans by 2017 [65]. Chen's group also summarized the development and application of glycosyltransferases until 2021 [53]. A few new glycosyltransferases [66–68] relevant to cell labeling have been reported in the last two years, with more attention being paid to improving performance [69] and expanding substrates [70] and applications [71–76]. The technique faces several challenges: glycosyltransferases that can tolerate unnatural monosaccharide donors are difficult to find; unnatural monosaccharide derivatives are more difficult to synthesize than the unnatural sugars of MGL; and chemoenzymatic labeling techniques are only suitable for reporting steady-state glycosylation and not for monitoring dynamic glycosylation.

Indeed, there is another class of glycosyl oxidases that can remodel specific glycosyl groups on the cell surface, and the resulting chemical groups can be labeled by bioorthogonal coupling. For example, galactose oxidase (GAO) is a copper metalloenzyme that oxidizes galactose/acetylgalactosamine (Gal/GalNAc) based on a free radical mechanism [77]. It is also possible to label a wider range of glycoforms by altering the substrate suitability of GAO through directed evolutionary techniques [78,79]. GAO tagging of terminal galactose has long been used for glycomics studies [80]. In addition, Ju's group used GAO oxidation, combined with chemiluminescence, to image terminal galactose in living cells [81].

Ding's group developed a series of GAO-based methods for oxidative remodeling of Gal/GalNAc at different spatial levels [82–87]. To ensure spatial specificity of glycan remodeling, they used potassium ferricyanide to inhibit GAO activity and potassium

ferrocyanide to activate GAO activity after the recognition process was completed. Based on this strategy, glycan remodeling of specific proteins in cells [82,84,85] and exosomes [86] was achieved. Tao et al. covalently modified cholera toxin B subunit (CTxB), which can specifically bind lipid rafts with GAO on the surface of gold nanoparticles, which allowed labeling and imaging of Gal/GalNAc in the lipid raft regions on the cell surface through spatiotemporal control of GAO activity (Figure 4) [83].

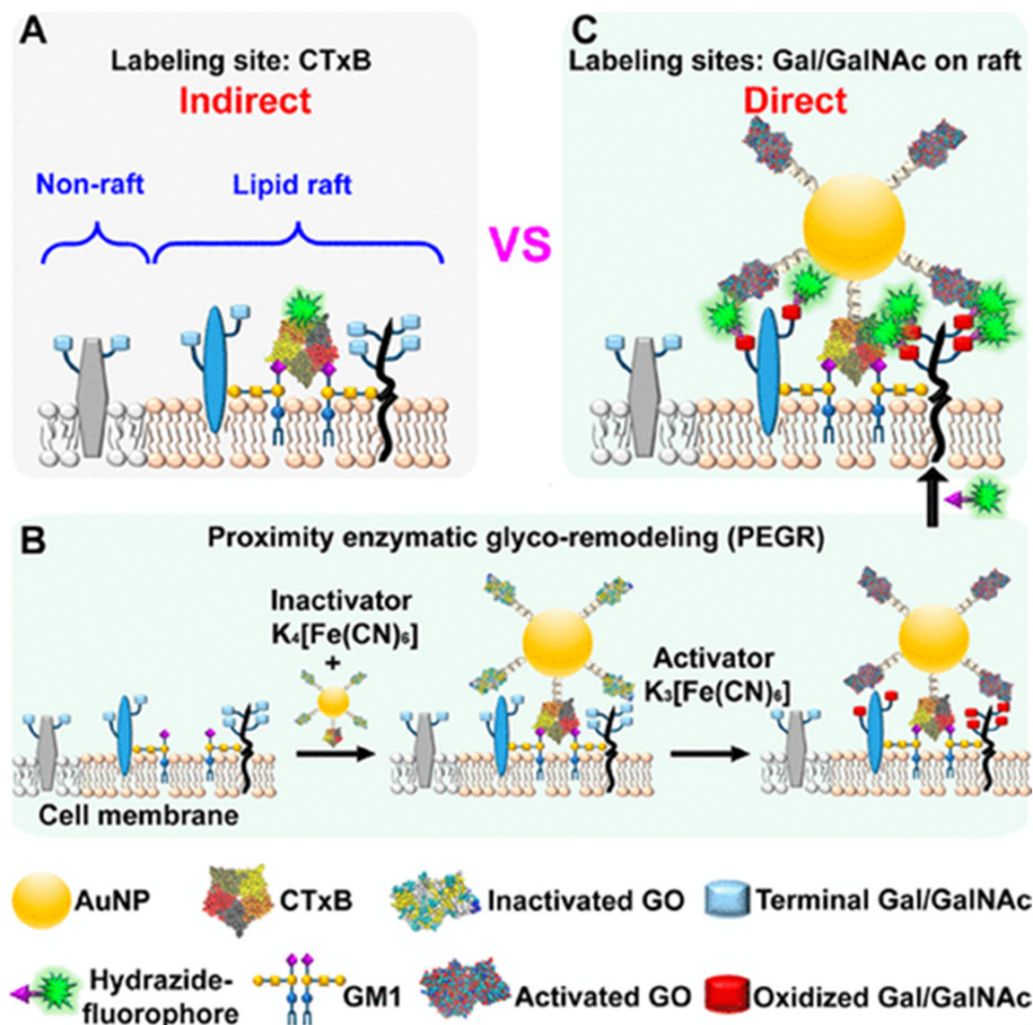


Figure 4. (A) Scheme of traditional fluorescence methods capable of recognizing lipid raft regions. (B,C) Schematic of covalent labeling of glycans in lipid rafts using CTxB to direct the localization of GAO to rafts [83]. AuNP, gold nanoparticle; CTxB, cholera toxin subunit B; and GO, galactose oxidase. Reproduced with permission from 83; published by the American Chemical Society, 2020.

In order not to directly interfere with the enzyme's activity, they encapsulated GAO using metal-organic framework (MOF) materials or polyethylene glycol (PEG) molecules to modulate the accessibility of the enzyme's active site. Zhang et al. encapsulated GAO in a MOF structure (ZIF-8) and loaded aptamers on the resulting GO@ZIF-8 to target specific tumor cells. Cell-selective Gal/GalNAc oxidation and imaging were achieved by disrupting the MOF structure with ethylene diamine tetraacetic acid (EDTA) after recognition (Figure 5) [82]. Li et al. covalently modified PEG containing disulfide bonds on the surface of GAO. After recognition of specific proteins, the disulfide bonds were cleaved using tris(2-carboxyethyl)phosphine (TCEP), allowing the PEG chains to be released and the GAO to access the glycans on the cell surface (Figure 6) [85].

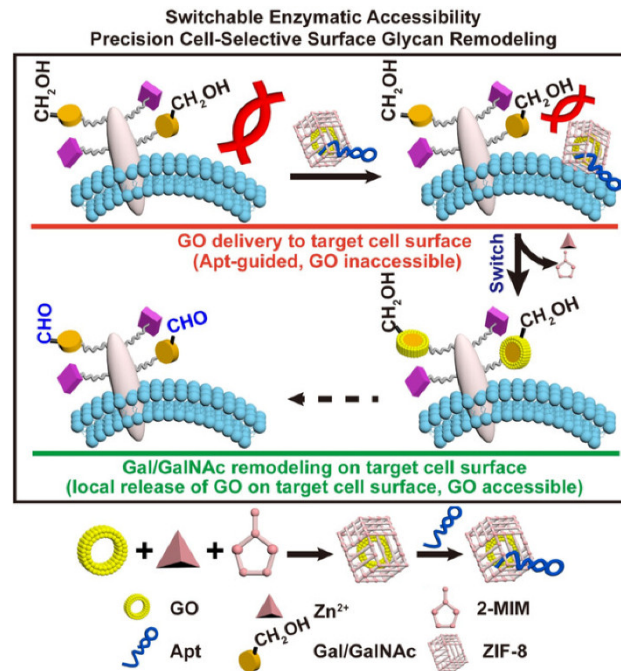


Figure 5. Schematics of switchable enzymatic accessibility strategy for precision cell-selective surface glycan remodeling [82]. GO, galactose oxidase; 2-MIM, 2-methylimidazole; Apt, aptamer; and ZIF-8, zeolitic imidazolate framework-8. Reproduced with permission from 82; published by Wiley Online Library, 2019.

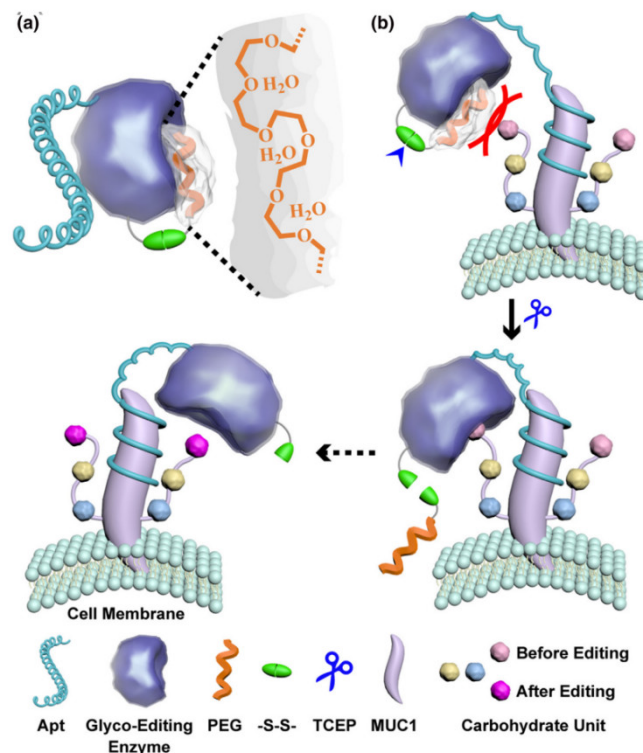


Figure 6. Schematic illustration of the localized enzyme decaging strategy for regulating enzyme activity used in protein selective labeling. (a) The glyco-editing enzyme is caged with PEG and modified with an aptamer to yield the probe. (b) After the probe specifically binds to the target protein, the PEG on the probe is cleaved by TCEP, exposing the enzyme active site and allowing protein specific glycan editing [85]. PEG, polyethylene glycol; TCEP, tris(2-carboxyethyl)phosphine

hydrochloride; and MUC1, mucin 1. Reproduced with permission from 85 published by Elsevier, ScienceDirect, 2021.

3.3. Chemical Covalent Labeling

In addition to the above methods, chemical covalent labeling using small molecules is a simple and rapid strategy for in situ studies of cellular glycans. Two approaches are commonly used, one based on the reversible reaction of phenylboronic acid with cis-dihydroxyl groups and the other based on the selective oxidation of sialic acids using sodium periodate at low temperatures.

Kataoka et al. evaluated the binding ability of sialic acids to phenylboronic acid (PBA) in aqueous solution at different pHs [88], which raised interest in PBA for detecting or labeling sialic acid on cells [89,90]. Matsumoto and co-workers employed fluorescently modified boronic acid to target multiple cancer stem cell subpopulations in parallel (Figure 7) [91]. Qualls et al. designed bis-boronic acid liposomes to recognize carbohydrates for selective labeling of diseased cells [92]. In general, the lower the pKa of the boronic acid ligand, the stronger the binding to cis-dihydroxyl groups. To improve the binding capability of boronic acid to carbohydrates, the introduction of tertiary amine groups, which can form intramolecular coordination with boron atoms (i.e., to form Wulff-type PBAs), to the adjacent positions of the boronic acid ligand [93,94] or the introduction of an intramolecular B-O coordinating group on the benzene ring [95,96] can reduce the pKa of the boronic acid ligand. However, the increased binding often leads to a decrease in glycan binding selectivity. How to find a balance between the two is something to think about. Although the specificity and stability of the reaction between boronic acid and sialic acid need to be improved, this is still a simple and rapid method for labeling carbohydrates.

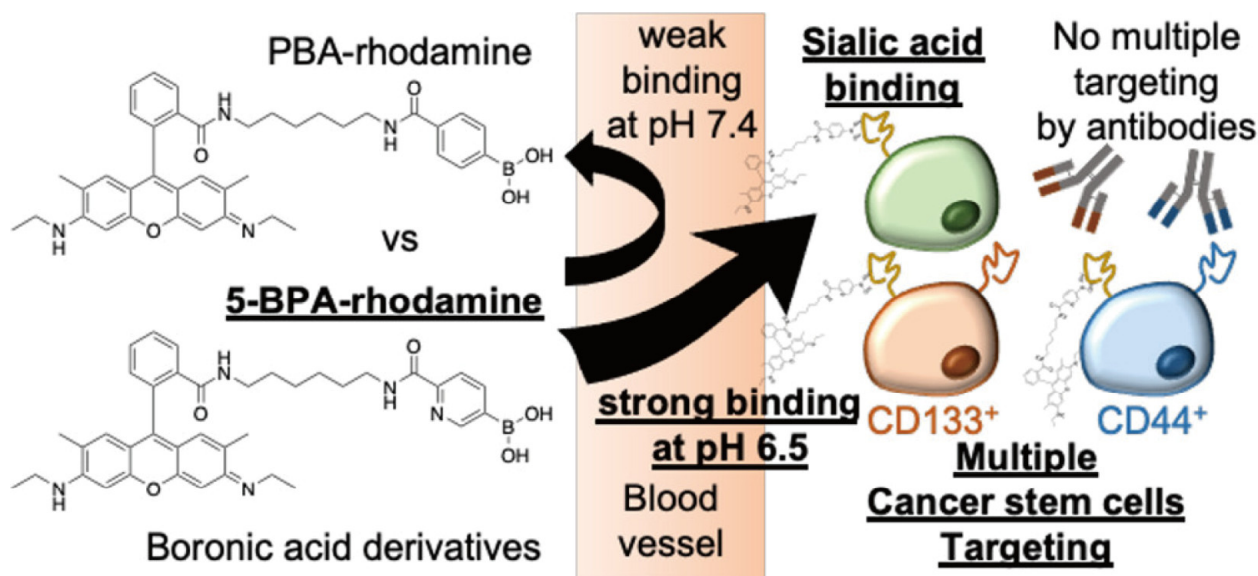


Figure 7. Schematic representation of pH-regulated fluorescence-modified 5-boronopicolinic acid (5-BPA) recognition for various cancer cells [91]. Reproduced with permission from 91 published by the American Chemical Society, 2021.

The oxidation of glycans using sodium periodate is a classical chemical reaction [97], and the low concentration and temperature conditions make it possible to selectively oxidize sialic acids on the living cell surface [98]. The aldehyde groups generated can be coupled with nanomaterials to achieve signal amplification [99,100]. Meanwhile, studies on the detection of sodium periodate-oxidized sialic acids on specific proteins have also been reported. Using a localized glycan labeling strategy similar to that of Ding's group, Sun et al. first identified the target protein with a protein probe containing an aptamer and a DNAzyme. Then, they oxidized cell-surface sialic acids with sodium periodate and

coupled a DNA-containing peptide beacon probe with bifunctional PEG. The proximity of the protein probe and peptide beacon probe, when they are on the same protein, can hybridize with each other, and the peptide beacon was released by the DNAzyme with the help of metal cofactors. The free protein probe can hybridize with the next adjacent beacon probe to achieve cyclic release of the labeled beacon. This strategy allows quantification of the beacon probe with HPLC and thus the abundance of labeled sialic acids. This sensing method converted sugar signals into peptide beacons, providing a novel quantification method for protein-carried glycans [101].

Comparing the two labeling methods for sialic acids: (1) Arylboronic acid labeling requires only a 1-step reaction, while periodate labeling requires 2 steps. (2) Arylboronic acid labeling requires careful pH adjustment to ensure label specificity, whereas periodate labeling requires careful control of sodium periodate concentration and reaction temperature. (3) Arylboronic acid labeling can be used for in vivo scenarios.

4. Glycan-Specific Sensing

The key to in situ sensing of glycans is the use of non-covalent recognition or covalent labeling methods to convert glycan signals at the cell surface into output signals such as force, light, electricity, or mass. These sensing strategies provide a faster and more sensitive means to detect complex glycosylation modifications on cell surfaces, which can help to track and understand glycan-related biological processes in situ. There is a wide variety of sensing techniques for cellular glycans, and we divide them here into two main categories according to whether they require labeling or not: Methods that do not require labeling mainly include surface plasmon resonance (SPR) and atomic force microscopy (AFM). They allow the study of glycan-related interactions at the molecular level and can quantitatively respond to the dynamics of glycan binding to different glycan-recognizing molecules under different conditions. Labeling methods include optical, electrochemical, and mass spectrometric techniques. These techniques allow either highly sensitive quantitative detection or in situ imaging of glycans on cells, which are summarized in Table 3. In addition, biomolecular layer interferometry (BLI) [102,103], microscale thermophoresis (MST) [104,105], lectin histochemistry [106–109], and enzyme-linked lectin assay (ELLA) [110,111] are also powerful tools for studying glycan recognition. However, these techniques are rarely applied to in situ sensing at the cell surface and are therefore not included in this review.

4.1. Surface Plasmon Resonance

Glycans are involved in a wide range of biorecognition processes, and the study of glycan interactions helps us better understand the communication events of living systems. The main types of glycan recognition include glycan–glycan interactions and glycan–protein interactions. SPR is commonly a labeling-free technique that can monitor glycan interactions in real time. Zhou’s group has conducted detailed work on the measurement of cell-surface glycan interactions. They designed a dual-channel substrate using SPR microscopy to solve nonspecific adsorption using a microfluidic device. One channel with poly-L-lysine deposited was used for cell immobilization, and the other channel with PEG covered was for reference. Parts of these two channels can be easily positioned in the field of view of an SPR microscope [112] and used for studying the interaction between lectins and glycans (Figure 8). They assessed wheat germ agglutinin (WGA) affinity towards N-acetylglucosamine and N-acetylneuraminic acid on human foreskin fibroblast (HFF) cells. This is the first study reporting on the binding and kinetic parameters of WGA interactions with two different glycosylated sites. They also studied the interaction of lectins with glycans in living and fixed cells [113]. Luo et al. [114] developed a localized surface plasmon resonance (LSPR) method using U-shaped gold nanoparticle (AuNP)-modified optical fibers. The sensitivity was significantly improved compared to the conventional SPR technique. Based on this technique, they performed in situ detection of cell-surface N-glycans with high sensitivity and a limit of detection of 30 cells/mL.

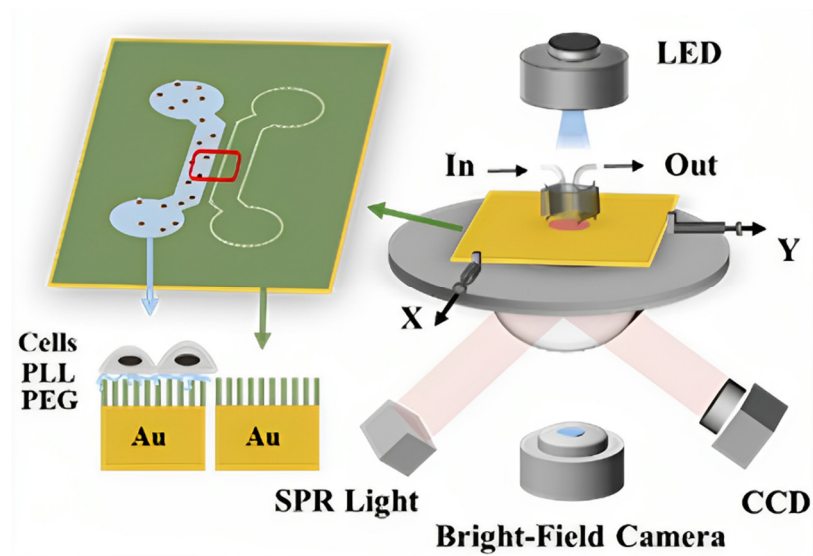


Figure 8. SPR microscope for measurement of cellular glycan–lectin interaction [112]. Red box shows the imaging area. PLL, polylysine. Reproduced with permission from 112 published by the American Chemical Society, 2022.

4.2. Atomic Force Microscope (AFM)

Alsteens's group employed AFM to investigate the binding of reovirus protein and sialic acids [115], and they have conducted extensive and rewarding research on the interaction of viruses with cellular glycans [116,117]. Otsuka and co-workers decorated a boronic acid-end-functionalized poly (ethylene glycol) onto an AFM cantilever, providing a dynamic and sialic acid-specific imaging mode [118] (Figure 9). Unlike conventional fluorescence microscopy and immunoelectron microscopy methods, their technique does not require pretreatment with glycan labeling. This feature suggests the possibility of analyzing living cells to reveal their true dynamics of glycosylation.

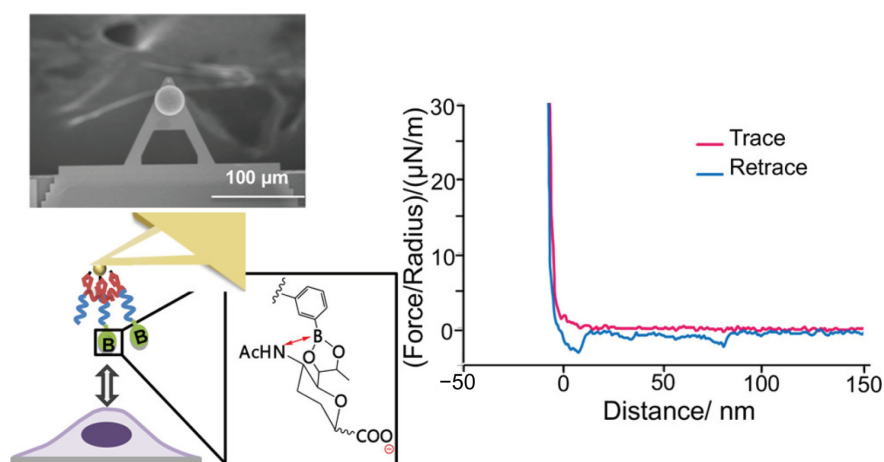


Figure 9. Schematic representation of AFM functionalized with boronic acid for dynamic imaging of sialic acids [118]. Reproduced with permission from 118 published by the American Chemical Society, 2020.

4.3. Optical Detection

Optical sensing is an analytical approach that converts the signals of glycans into recognizable optical signals, including fluorescence, surface-enhanced Raman scattering (SERS), chemiluminescence (CL), etc. These approaches facilitate the quantitative analysis and imaging of cell-surface glycans.

4.3.1. Fluorescence

After fluorescent labeling, the glycans can be easily quantified using flow cytometry, which has the capability of multi-parameter analysis. Fu et al. performed flow cytometric quantitative analysis of PD-L1-specific sialic acids on the cell surface by designing a proximity ligation assay (PLA)-mediated rolling circle amplification strategy, which effectively amplified the fluorescence signal of PD-L1's glycans, thus improving the detection limit [119]. Ding et al. applied flow cytometry to the terminal galactose and sialic acids on the sperm surface using glycan oxidation labeling [120]. The authors found that the glycosylation level of spermatozoa from diabetic mice was higher than that of the normal group, revealing the relationship between glycosylation modification and sperm quality, thus laying the foundation for the development of glycan-related reproductive markers.

In addition to flow cytometry-based strategies, lectin arrays are a very classical technique for in situ fluorescence analysis of cellular glycans [121–124]. After incubation of fluorescently labeled cells with microarrays modified with a variety of lectins, the number of cells captured on different lectin blots is used to reflect the glycosylation of the cells. To increase sensitivity, this mode can be reversed by immobilizing the cells on the surface of a specific substrate, then incubating a tagged lectin and using the tag on the lectin to dock to a signal amplification module. Feng et al. [125] constructed an exosome array and amplified the glycan signals by initiating a DNA rolling circle amplification based on the recognition of exosome surface glycans via lectins. In situ detection of multiple cancer-associated glycans on the exosome surface was achieved using different lectins at different locations (Figure 10).

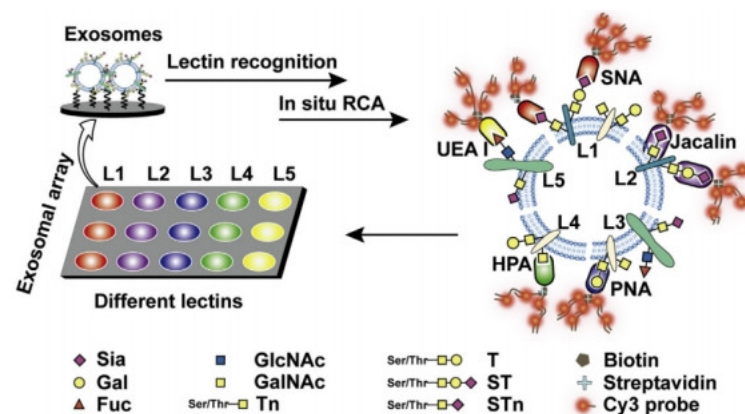


Figure 10. Schematic illustration of the lectin-mediated RCA signal amplification strategy for in situ detection of exosomal glycans [125]. RCA, rolling circle amplification. Reproduced with permission from 125 published by Elsevier, ScienceDirect, 2018.

The fluorescence resonance energy transfer (FRET) process is strongly dependent on the distance between the fluorescent donor and the receptor and was thus the first technique used for protein-specific glycan imaging. Currently, FRET-based methods for glycan analysis have been widely reported [126–129]. For example, Chen et al. [130] developed two probes and an exonuclease III-assisted recycling hybridization strategy for quantitative fluorescence analysis of the glycans of the target protein on the cell surface (Figure 11). The researchers constructed two DNA sequence-based probes, a protein probe (PP) and a glycan probe (GP), where PP consists of an aptamer and a DNA sequence partially complementary to GP, whereas GP mainly consists of a fluorophore and a quencher, as well as a DNA sequence partially complementary to PP. The GP probe is first labeled for cellular glycans using the metabolic labeling technique. To distinguish the target glycans on the given protein, PP is added to bind to the protein. Hybridization of PP with the adjacent GP probe can trigger cleavage of the GP probe by enzyme exonuclease III, releasing the fluorophore and returning the PP probe to its free state. Subsequently, the PP probe continues to hybridize with other GP probes on the bound protein, thereby converting the

individual glycans on the target protein into fluorescent signals. Using this method, the authors successfully achieved sialic acid imaging of EpCAM on the surface of MCF-7 cells, paving the way for in situ quantitative analysis of protein-specific glycans.

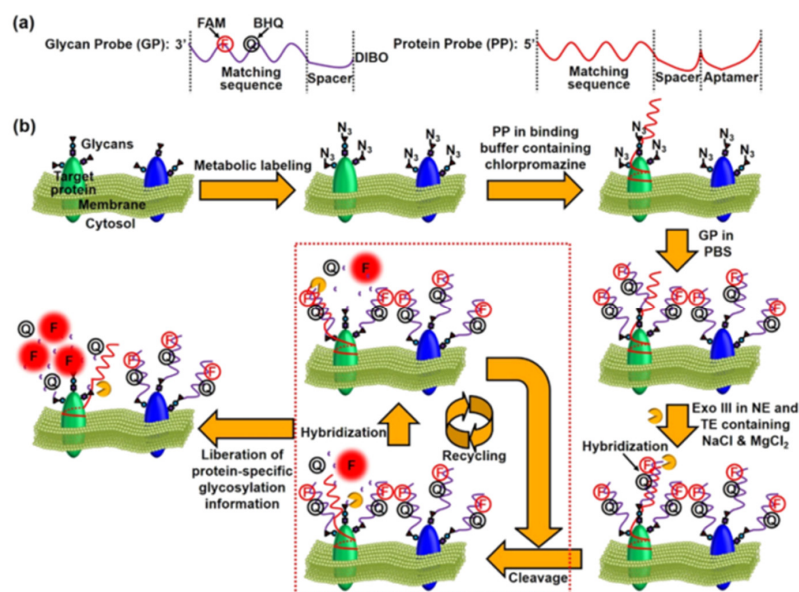


Figure 11. Schematic illustration of (a) the glycan probe (GP) and protein probe (PP) (b) for in situ quantitative analysis of protein-specific glycans on the cell surface through a pair of probes and the exonuclease III-aided recycling hybridization strategy [130]. FAM, 6-carboxyfluorescein; BHQ, black hole quencher; DIBO, dibenzocyclooctyne-amine (DIBO); NE, nuclease buffer; and TE, tris-EDTA. Reproduced with permission from 130; published by the American Chemical Society, 2016.

Fluorescence methods can also be combined with other modalities to analyze glycans. Liang et al. [131] developed a dual-mode paper-based biosensor that integrates fluorescence and colorimetric sensing signals and further amplifies the signals through the multibranching hybridization chain reaction (mHCR) (Figure 12). In this approach, *concanavalin A* (Con A), a lectin that targets cell-surface glycans, was combined with mHCR. PtCu nanochains and graphene quantum dots (GQDs) were attached to long chains generated by mHCR to form the nanoprobe for signal amplification. Aptamer was used to capture cells on the surface of Ag-Au microfluidic paper-based analytical devices (μ PADs), followed by Con A-guided binding of the nanoprobe. In the probe, GQDs were used to generate fluorescent signals, and the peroxidase-like activity of PtCu nanochains catalyzed 3,3',5,5'-Tetramethylbenzidine (TMB) to produce a colorimetric signal, enabling highly sensitive bimodal visual detection of cell-surface N-glycans.

4.3.2. Surface-Enhanced Raman Scattering (SERS)

Surface-enhanced Raman scattering (SERS) is an analytical technique that utilizes the enhancement of Raman scattering signals on nanostructured surfaces [132]. When molecules adsorb onto specific metal nanoparticles or nanostructured surfaces, it results in a significant enhancement of Raman scattering signals, providing high sensitivity for analysis [133], and has been extensively applied in biological analysis [134]. Although there have been numerous reports on the detection of saccharides using SERS [135–138], the majority of these methods are focused on in vivo analysis and cannot achieve in situ quantification. Chen et al. [139] proposed a micro-competition system that combines dual-surface monolayer competition with SERS for simultaneous quantification of multiple polysaccharides on the intact cell surface. In this design (Figure 13), gold nanoprobe were prepared by coating different Raman-active molecules and lectins onto gold nanoparticles, allowing both SERS signal resolution and glycan recognition. The silica bubbles functionalized with multi-polysaccharide-coated gold nanostars act as artificial polysaccharide

surfaces and SERS substrates to compete with the cells for the gold nanoprobes. This micro-competition system enables the simultaneous detection of multiple polysaccharides on the intact cell surface via SERS quantification of different gold nanoprobes on the silica bubbles. This method solves the challenge of simultaneously quantifying multiple glycans in intact living cells.

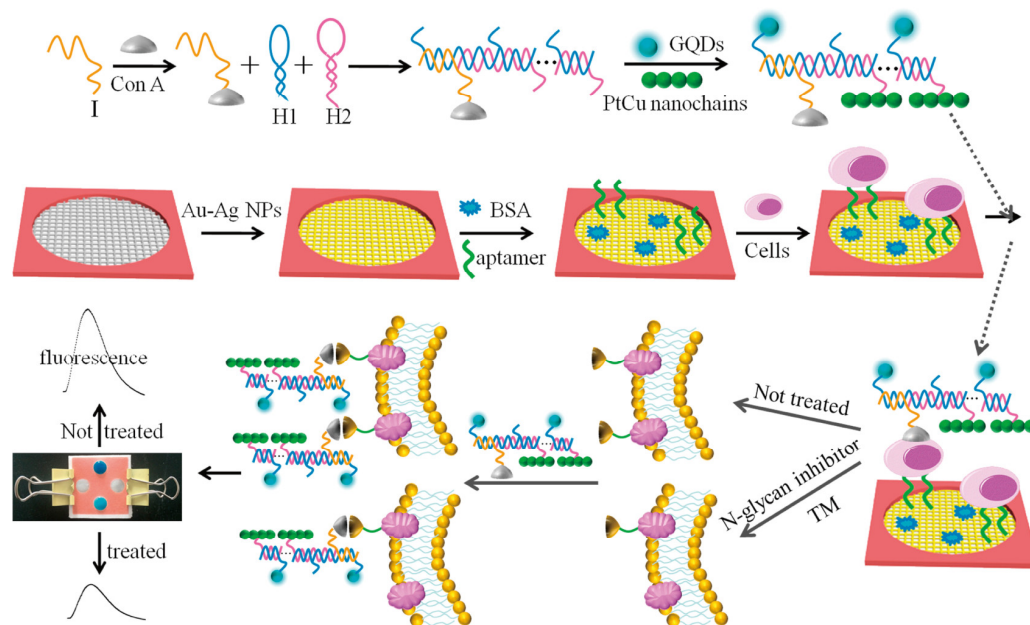


Figure 12. Schematic representation of a dual-mode paper-based biosensor for real-time monitoring of cell-surface glycans using fluorescence and colorimetric sensing signals [131]. I, initiating chain; H1, hybrid chain 1; H2, hybrid chain 2; GQDs, graphene quantum dots; and TM, tunicamycin. Reproduced with permission from 131 published by Elsevier, ScienceDirect, 2016.

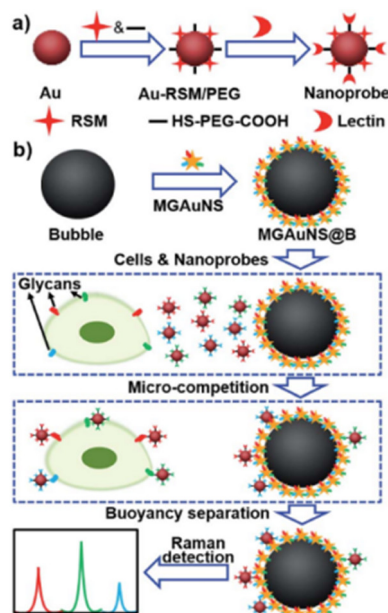


Figure 13. Schematic illustration of (a) nanoprobe synthesis and (b) design of the micro-competitive system involving gold nanoprobes, silica bubbles, and target cells for in situ detection of cell-surface glycans using SERS [139]. RSM, Raman signal molecule; MGAuNS@B, multiple-polysaccharide-coated gold nanostars. Reproduced with permission from 139 published by the Royal Society of Chemistry, 2015.

The enhancement of Raman scattering signals plays a key role in highly sensitive detection. Nanotags are typically composed of nanomaterials with high Raman activity and a high surface area, both of which enhance the intensity of Raman signals and have garnered significant attention in the SERS detection of trace substances [140,141]. Cordina et al. [142] employed SERS nanotags functionalized with lectins to enhance Raman signals for specific detection of glycoproteins on cell surfaces (Figure 14). Using immunoglobulin G (IgG) as a model, the surface glycans of IgG as low as 10 ng IgG in one drop (1 μ L) could be detected within two hours. To further enhance the SERS activity and stability of the nanotags, Miao et al. [143] successfully synthesized nitrogen-doped graphene quantum dots (NGQDs) with exceptional long-term stability and biocompatibility, resulting in an effective enhancement of Raman activity. Subsequently, they conjugated NGQDs with 4-mercaptophenylboronic acid (MPBA) for cell-surface glycan sensing. This method demonstrated excellent selectivity and sensitivity.

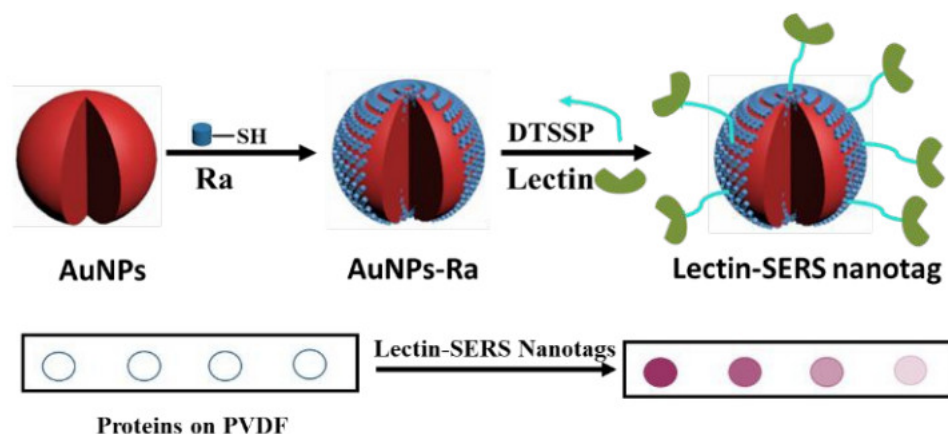


Figure 14. Schematic illustration of the lectin-modified nanotags for enhancing SERS activity in the detection of cell-surface glycans [142]. Ra, Raman reporter; DTSSP, 3,3'-dithiobis[sulfosuccinimidyl]propionate; and PVDF, polyvinylidene fluoride. Reproduced with permission from 142 published by the Royal Society of Chemistry, 2020.

4.3.3. Other Optical Methods

In addition to the common methods mentioned above, there are other techniques that can be used for in situ detection of cell-surface glycans. Chemiluminescence (CL) is a phenomenon in which luminescent substrates, through chemical reactions, generate excited-state molecules that emit visible or ultraviolet light upon returning to their ground state. The most important features of this technique are the absence of excitation light and the low background signal. Han et al. [81] combined chemoselective labeling of glycans with chemiluminescent array detection to achieve simultaneous analysis of two types of glycans on cells. They oxidized cell-surface Gal/GalNAc and sialic acids to generate aldehyde groups and then covalently coupled avidin. They then bind gold nanoprobe loaded with biotin and a large amount of horseradish peroxidase (HRP) to the avidin. HRP can catalyze luminal- H_2O_2 chemiluminescence, enabling in situ monitoring of cell-surface sialic acids and Gal/GalNAc, and the detection limit can reach as low as 12 cells.

With the continuous progress of new technologies, in situ detection methods of cell-surface glycans are becoming more diversified. Liu et al. [144] proposed a novel photoacoustic detection system for signal amplification that enabled in situ detection of the glycosylation of mucin 1 in mice with breast cancer. This study provides a new idea for monitoring glycosylation in vivo.

4.4. Electrochemical Detection

An electrochemical biosensor is a device that uses changes in electrical signals (e.g., current, electrode potential, electrochemical impedance, etc.) generated by the binding of a

biomolecule to the surface of an electrode for analysis [145]. Electrochemical methods have been widely used for the detection of cell-surface glycans because of their rapid response, high sensitivity, and ease of quantification [146]. Another major advantage of electrochemical methods over other methods (AFM, fluorescence microscopy, flow cytometry, mass spectrometry, etc.) is that the devices are inexpensive and easy to miniaturize.

The generation of electrochemical signals is closely related to the electron transfer process at the electrode surface, and efficient electron transfer contributed to increased detection sensitivity. Therefore, researchers have worked to develop and apply novel conductive materials and methods to electrochemical analysis to improve electron transfer efficiency. These materials include ferrocene [147], silver nanoparticles (AgNPs) [148], Cu-based metal-organic frameworks (Cu-MOFs) [149], reduced graphene oxide (rGO) [150], Pd@Au NPs [151], single-wall carbon nanotubes (SWNTs) [152], and multi-walled carbon nanotubes [153]. Organic electrochemical transistors (OECTs), an emerging device, are a unique class of organic thin-film transistors (OTFTs). They can operate at lower voltages and regulate charge transport through electrochemical reactions, allowing stable operation under low-voltage conditions [154]. OECT-based biosensors have been employed for the detection of cell-surface glycans [149,155–158]. Chen et al. [159] constructed an electrochemical biosensor based on mercaptopropionic acid (MPA)-modified OECT and successfully achieved quantitative detection of cell-surface glycans. In this study, an HRP-lectin probe was used to recognize cell-surface glycans. Upon binding the probe to cell-surface glycans, HRP catalyzed the decomposition of H_2O_2 , inducing electron transfer in the OECT and generating an electrical signal. Additionally, the intensity of the electrical signal was directly proportional to the amount of glycans.

In addition to the use of novel conductive materials, the detection sensitivity can be improved by introducing signal amplification methods [160–162]. Qian et al. [161] utilized single-walled carbon nanohorns (SWNHs) for signal amplification, and these SWNHs hold a larger surface area that can accommodate considerable reactive sites, resulting in the amplification of differential pulse voltammetry (DPV) signals. Zhang et al. [163] combined the amplification effect of multi-walled carbon nanotube/Au nanoparticle (MWNT/AuNP) materials with the excellent catalytic performance of HRP to achieve signal amplification. Ding et al. [164] prepared a nanohorn scaffold functionalized with arginine-glycine-aspartic acid-serine tetrapeptide on the electrode surface for cell capture and enhancing electron conduction (Figure 15). A lectin- and HRP-co-functionalized gold nanoprobe was also developed for dual signal amplification of electrochemical signals based on enzymatic catalysis and the high surface-to-volume ratio of gold nanoparticles. The study enabled highly sensitive and selective in situ assessment of cell-surface glycans, with a detection limit of as low as 15 cells.

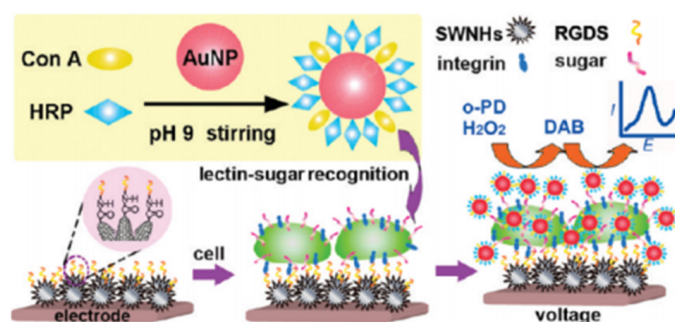


Figure 15. Schematic illustration of a tetrapeptide nanohorn scaffold for enhancing electron transfer and cell capture, which enables the highly sensitive detection of glycans in situ combined with a gold nanoprobe [164]. HRP, horseradish peroxidase; AuNP, gold nanoparticle; SWNHs, single-walled carbon nanohorns; RGDS, arginine-glycine-aspartic acid-serine tetrapeptide; *o*-PD, *o*-phenylenediamine; and DAB, 2,2'-diaminoazobenzene. Reproduced with permission from 164 published by the American Chemical Society, 2010.

Electrochemiluminescence is a unique electrochemical phenomenon involving the coupling of redox reactions and luminescence reactions within an electrochemical system. Many studies employed electrochemiluminescence for the detection of cell-surface glycans due to its high sensitivity and low background interference [165–168]. Han et al. [165] employed a variant of the “one molecule-two surfaces” competition format to realize in situ label-free analysis of cell-surface carbohydrates. They immobilized mannan-functionalized CdS quantum dots on the electrode to compete with cell-surface glycans towards Con A. In the absence of cells, Con A is captured using mannan on the electrode surface, resulting in blocked electron transfer and a weak electrochemiluminescence signal. In the presence of cells, the amount of mannan-captured lectin on the electrode decreases, resulting in less electron transfer blockage and the restoration of the electrochemiluminescence signal. The major advantage of this strategy is that it reflects the glycan level across the entire cell surface and does not require pre-modification of cells or lectins (Figure 16).

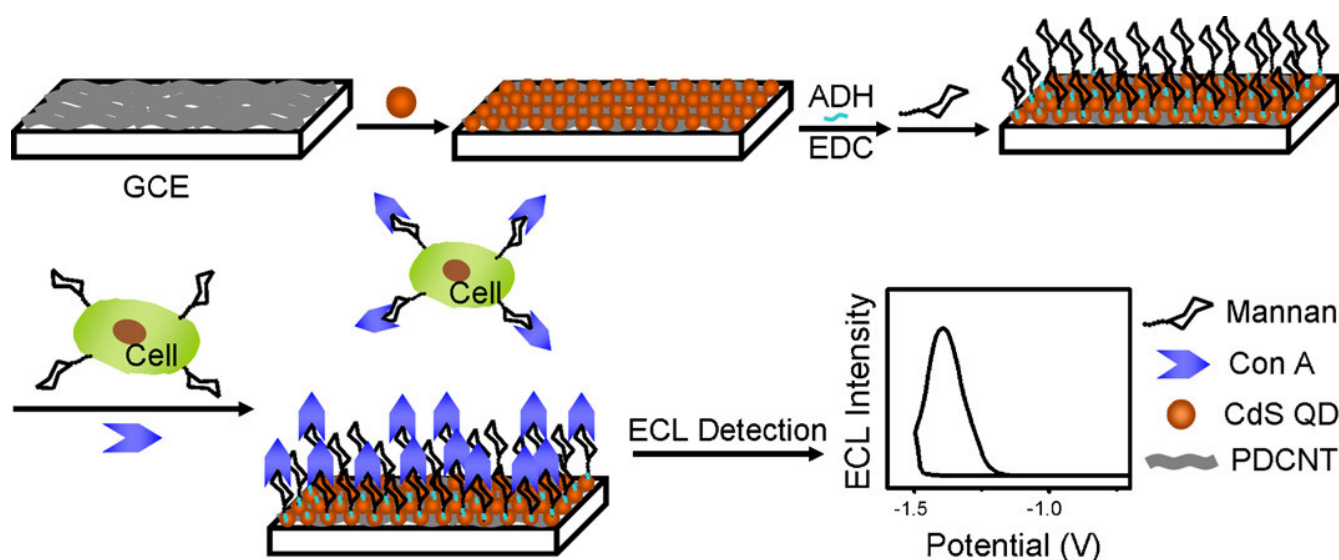


Figure 16. Schematic representation of the label-free in situ analysis of cell-surface glycans, which was achieved by modulating the electrochemiluminescence output signal through competitive binding [165]. GCE, glassy carbon electrode; ADH, adipic dihydrazide; EDC, 1-(3-dimethylaminopropyl)-3-ethylcarbodiimide hydrochloride; QD, quantum dot; and PDCNT, poly (diallyldimethylammonium-functionalized multi-walled carbon nanotube). Reproduced with permission from 165 published by Elsevier, ScienceDirect, 2011.

Chen et al. [169] designed sandwich electrochemiluminescence biosensors for dynamic assessment of cell-surface N-glycans. They modified Con A on the electrode surface to capture cells. They also designed a probe composed of Con A-functionalized gold nanoparticles (AuNPs) and silica nanoparticles containing $\text{Ru}(\text{bpy})_3^{2+}$ for the recognition of cell-surface N-glycans. This scaffold was able to enhance electrochemiluminescence signals with detection limits as low as 600 cells/mL.

The team then redesigned the detection elements. Using the high loading capacity and electron transfer efficiency of poly(amidoamine) (PAMAM) and reduced graphene oxide (rGO), the number of cells captured was increased, and signal amplification was achieved. At the same time, AuNPs were used to load alkaline phosphatase (ALP) and Con A, where Con A can recognize N-glycans on the cell surface and ALP can produce phenol under AuNP-based catalysis, which can inhibit the electrochemiluminescence reaction of $\text{Ru}(\text{bpy})_3^{2+}$. The detection of glycans on the surface of cancer cells can be realized by monitoring the signal attenuation after probe binding. This method has excellent detection sensitivity, and the detection limit is reduced to 38 cells/mL [170] (Figure 17).

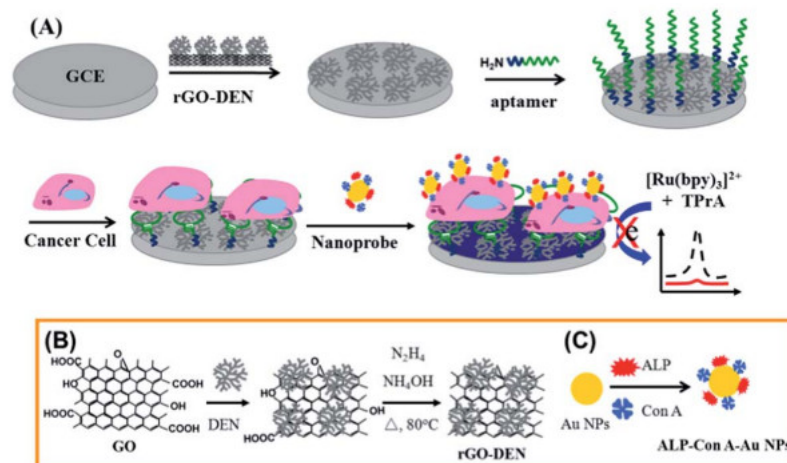


Figure 17. (A) Schematic illustration of electrochemiluminescence biosensor utilizing aptamers, employing multivalent recognition and ALP-responsive signal amplification, for highly sensitive cell detection and assessment of cell-surface carbohydrates. (B) The production process of rGO-dendrimer conjugates. (C) Steps involved in creating ALP-Con A-AuNPs nanoprobes [170]. ALP, alkaline phosphatase; rGO, reduced graphene oxide; TPrA, tripropylamine; and DEN, dendrimer. Reproduced with permission from 170 published by the Royal Society of Chemistry, 2014.

4.5. Mass Spectrometry (MS)

Mass spectrometry (MS) is a reliable qualitative and quantitative analytical method with irreplaceable advantages in glycan analysis and has been widely used to determine glycan structures and glycosylation sites. Common mass spectrometry techniques used for cell-surface glycan analysis include electrospray ionization mass spectrometry (ESI-MS) [171], laser desorption/ionization mass spectrometry (LDI-MS) [172,173], etc. The use of mass spectrometry for the in situ analysis of cell-surface glycans has attracted the attention of researchers because of the potential loss of the spatial distribution information of cellular glycans due to sample pretreatment involved in conventional mass spectrometry analysis [174,175]. Unlike strategies in glycomics, in situ mass spectrometry glycan analysis methods generally use glycan labeling/recognition techniques to introduce mass tags on the target glycans, which are then released and detected during MS detection. Advantages of this type of strategy include high ionization efficiency, ease of simultaneous detection of multiple glycans on the cell surface (based on lectin recognition), high detection sensitivity, and the potential to further extend the methods to tissue sections. There are currently two main types of tag release techniques: laser-cleavage-assisted and enzyme-catalyzed-assisted.

4.5.1. Laser-Cleavage Assisted In Situ Detection

When the laser is directed at molecules, its high energy may induce the potential cleavage of chemical bonds, especially non-covalent bonds. For example, the hydrogen bonds between DNA duplexes were easily broken under laser irradiation. He et al. [176] encoded lectins with different DNA primers, which can produce long single-strand DNA (ss-DNA) with repetitive sequence units by rolling circle amplification and hybridizing with multiple short DNA probes. These lectin-DNA complexes can identify the corresponding glycans on the cell surface. Subsequently, the duplexes were broken upon laser irradiation, and the detached probes from cell surfaces were detected using matrix-assisted laser desorption/ionization mass spectrometry (MALDI-MS). However, nucleic acids are not ideal carriers for mass spectrometry tags, and the homogeneity of the matrix spray and the sample on the target plate can affect the quantitative results of mass spectrometry.

The covalent bond between the mass tags and the cellular glycans can also be designed to be cleavable via laser irradiation. Recently, laser-cleavable probes have attracted a lot of attention, which is generally based on the fact that the photocleavable C-S bond introduced

between the glycans and mass tags can be cleaved under 533 nm laser irradiation. Han et al. took advantage of this to design four types of laser-cleavable probes. By combining these probes with lectins, various glycans on the cell surface can be detected at the single-cell level via LDI-MS [177]. To improve detection sensitivity, Sun et al. [178] designed a method that integrates metabolic labeling and click reactions to efficiently attach more laser-cleavable probe molecules to the sialoglycoconjugates on the cell surface. The detection limit of this method is 5 fmol (Figure 18), which does not require enzymatic cleavage of glycans, has high sensitivity and throughput, and is universal for different glycans.

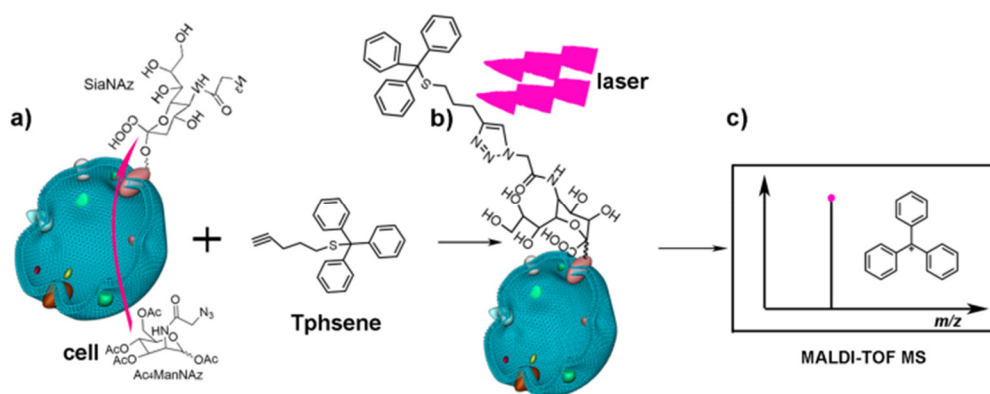


Figure 18. (a) Introduction of azido-sialic acid (azido-Sia) onto the cellular surface using Ac₄ManNAz-based biorthogonal chemistry. (b) Utilization of click chemistry for thiolene labeling/tagging with Tphsene. (c) MALDI-TOF MS measurement of MS beacons. [178]. Reproduced with permission from 178 published by the American Chemical Society, 2018.

Subsequently, Ma et al. [172] developed a simpler *in situ* glycan analysis strategy using dual-functional laser cleavable mass spectrometry probes (LCMPs). The LCMPs are synthesized by covalently linking lectins and molecular tweezers (MTs) to gold nanoparticles (Au NPs) through sulfur-containing bifunctional linkers. The lectins act as recognition units and specifically bind to glycan on the cell surface, while the MTs act as signal amplifiers and matrices in LDI-MS. The release of MTs from AuNPs was detected via LDI-MS under laser irradiation, enabling *in situ* analysis of cell-surface glycans.

4.5.2. Enzyme-Catalyzed Assisted *In Situ* Detection

Enzyme-catalyzed tag release is another strategy for *in situ* MS analysis of glycans. In this method, a synthetic peptide of a known sequence is labeled as a reporter peptide on the glycans of interest, and then the reporter peptide is detected via mass spectrometry using enzymatic digestion, which can reflect the number of glycans to be measured. The enzymatic process is characterized by high efficiency and site specificity.

Sun et al. [179] designed a two-probe method for *in situ* quantization of galactose/N-acetylgalactosamine (Gal/GalNAc) at the end of MUC1. The two probes are the protein probe and the glycan probe. The protein probe contained an aptamer-recognizing MUC1 and a segment for capturing DNA sequences, while the glycan probe featured a sequence complementary to the capture DNA, a peptide segment acting as a reporter peptide, and an enzymatic cleavage site. The glycans on the cell surface were linked with the glycan probe using the bioorthogonal labeling method. After protein probe identification, the reporter peptide on the glycan probe can be selectively released in the presence of exonuclease III, allowing quantitative determination of Gal/GalNAc. However, the operation process of this method is complicated, and the sensitivity is insufficient. DNAzyme motors are typically designed to achieve nanoscale mechanical motion in specific catalytic reactions, allowing the movement of the DNAzyme to the catalytic site for precise positioning. Liu et al. [101] constructed a metal-ion-regulated, recyclable DNAzyme motor based on a dual-probe approach for highly sensitive *in situ* detection of glycans. Through a hybridization or

hydrolysis process, it can detect all terminal sialic acid sites on the target protein. The cleaved reporter peptide is quantified using LC-MS after enzymatic catalysis (Figure 19).

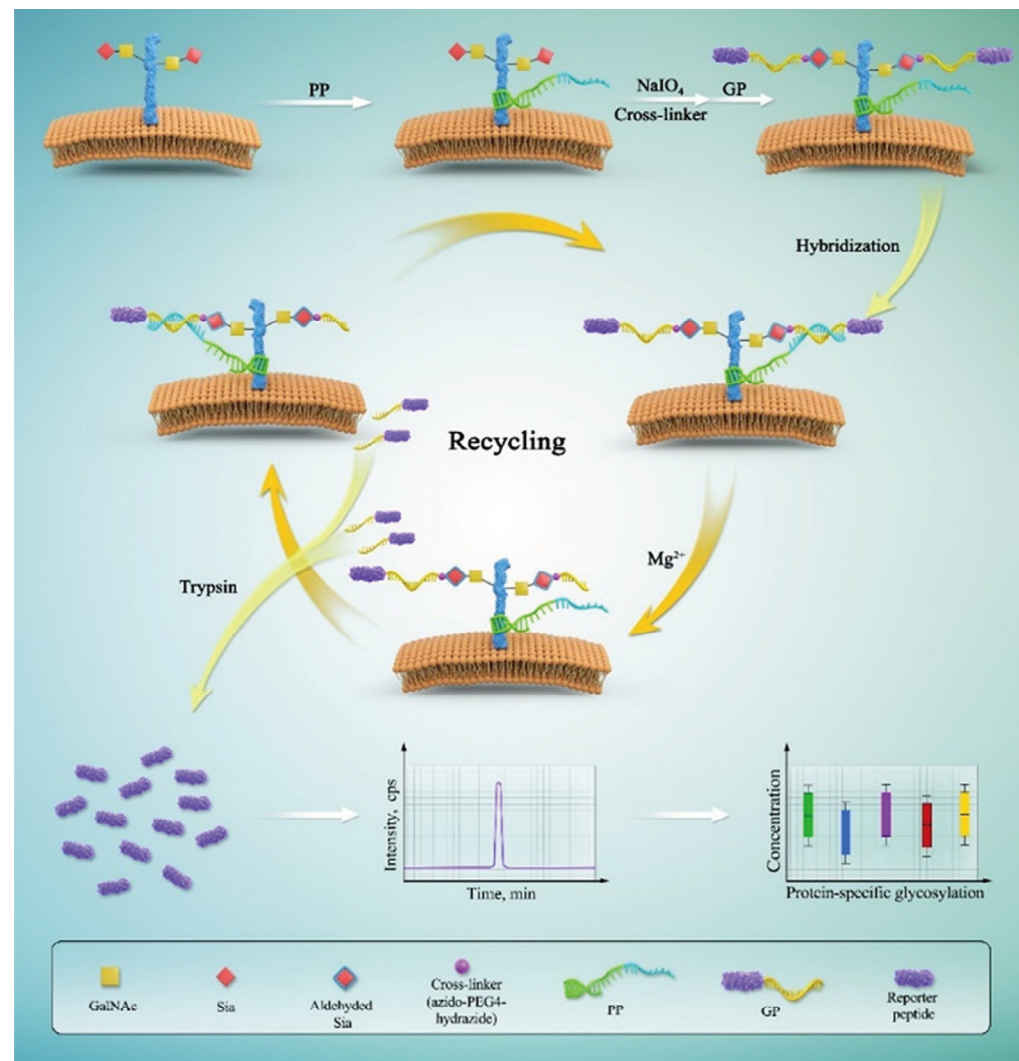


Figure 19. Schematic diagram of a dual-probe method based on a metal ion-regulated DNAzyme motor for highly sensitive detection of glycoproteins [101]. PP, protein probe; GP, glycan probe. Reproduced with permission from 101 published by the American Chemical Society, 2022.

Table 1. Recognition molecules for glycans.

Recognition Molecule	Name	Specificity	Labeling Strategy	Application	Ref.
Lectin	AAL	Fuc	Fluorescent nanodiamonds	Glycan targeting therapy	[23]
	ECA	Gal	Fluorescent molecule	Cellular localization of glycan residues	[24]
	SBA	GalNAc			
	BPL	GlcNAc			
	NPA	Man	Label-free	Cell-selective glycoform analysis	[25]
SSA	Sia				
	LTL	Fuc	Label-free	Detection of tumor cell vesicles	[26]

Table 1. Cont.

Recognition Molecule	Name	Specificity	Labeling Strategy	Application	Ref.	
Lectin	hMGL	Tn/sTn (GalNAc α 1-Ser/Thr, Sia α 2-3GalNAc α 1- Ser/Thr)	Label-free	Assessment of glycan–protein interactions	[30]	
	RCA120 Siglec-2-Fc	Gal, Lac Sia	Fluorescent molecule		[31]	
	WGA	GlcNAc	Label-free		[112]	
	UEA I SNA Jacalin PNA HPA	Fuc Sia Gal Gal GalNAc	DNA-fluorescence conjugate	Analysis of exosomal glycans of tumor cells	[125]	
	LCA WGA	Man GlcNAc				Nanoparticles
	Con A	Man	Nanoparticles, Mass tag	Quantification of cell-surface glycans	[164,165,169, 171,176,177]	
	Antibody	S0G0-GlcNAc2- Q β	GlcNAc	-	Antibody screening	[33]
		Anti CA19-9	CA19-9	Composite nanomaterial	Detection of CA19-9	[35]
		Anti-SSEA-1	Lewis x	Technetium-99m	-	[38]
		Anti-TF	TF (Gal β 1-3GalNAc α 1- Ser/Thr)	-	-	[40]
Anti- α -Gal (27H8)		Galili (Gal- α 1,3-Gal)	-	-	[41,42]	
IgM to the Forssman disaccharide		Forssman (GalNAc- α 1,3-GalNAc)	-	-	[42,43]	
Aptamer	SL-11	Sialyllactose	-	-	[47]	
	Apt9	Sialyllactose	Nanoparticles	-	[48]	
	Clone 5 RNA aptamer	Sialyl Lewis X	-	Inhibition of cell adhesion	[49]	
	TGP4	Biantennary digalactosylated disialylated N-glycan A2G2S2	Fluorescent molecule	Quantification of cell membrane glycans	[51]	

Aleuria aurantia lectin (AAL), Erythrina cristagalli agglutinin (ECA), Soybean agglutinin (SBA), Bauhinia purpurea lectin (BPL), Narcissus pseudonarcissus agglutinin (NPA), Sambucus sieboldiana agglutinin (SSA), Lotus tetragonolobus lectin (LTL), succinylated wheat germ agglutinin (WGA), Ulex Europaeus agglutinin I (UEA I), Peanut agglutinin (PNA), Sambucus Nigra lectin (SNA), Helix pomatia agglutinin (HPA), Lens culinaris agglutinin (LCA), Concanavalin A (Con A), Thomsen–Friedenreich glycoantigen (TF), Fucose (Fuc), Galactose (Gal), Lactose (Lac), N-acetylgalactosamine (GalNAc), Sialic acid (Sia), N-acetylglucosamine (GlcNAc), and Mannose (Man).

Table 2. Covalent labeling methods for glycans.

Covalent Labeling Method	Probe	Glycan	Application	Ref.
Metabolic glycan labeling	Ac ₄ Fuc ₇ Alk	Fuc	Fuc imaging	[57]
	1,3-Pr ₂ GalNAz	GalNAc	Identification of protein glycosylation	[58]

Table 2. Cont.

Covalent Labeling Method	Probe	Glycan	Application	Ref.
Metabolic glycan labeling	Ac ₄ ManAz	Sia	Sia imaging	[59]
	GlcNAz, GlcNAI	Polysaccharide E. coli K5	In vivo bacterial detection	[60]
	ManNAz 1,3-Pr ₂ ManNAz 1,6-Pr ₂ ManNAz	Sia	Avoiding S-glyco-modification and SA imaging	[62–64]
Chemoenzymatic glycan labeling	ST3Gal1	Sia (donor sugar)	Probing of the binding specificities of siglecs	[73]
	ST6Gal1	Sia (donor sugar)	Capturing glycan–protein interactions	[74]
	CgtA	GalNAc (donor sugar)	Investigation of the effects of pathogen invasion	[75]
	WbwK	Fuc (donor sugar)	TF detection and imaging	[76]
	Galactose oxidase	Terminal Gal/GalNAc	Gal/GalNAc quantification and imaging	[77–87]
Chemical covalent labeling	PBA	Sia	Sia quantification and imaging	[88–92]
	Wulff-type PBA	Lipopolysaccharide	Gram-negative bacteria detection	[93,94]
	BOB	Terminal Gal	Gal detection	[95,96]
	NaIO ₄	Sia	Sia quantification and imaging	[97–99]

7-Alkynyl-tetra-acetylated fucose (Ac₄Fuc₇Alk), 1,3-di-opropionyl-N-azidoacetylgalactosamine (1,3-Pr₂GalNAz), tetra-acetylated N-azidoacetylmannosamine (Ac₄ManAz), N-azidoacetyl-D-glucosamine (GlcNAz), N-pentynylacetylglucosamine (GlcNAI), 1,3-di-opropionyl-N-azidoacetylmannosamine (1,3-Pr₂ManNAz), 1,6-di-opropionyl-N-azidoacetylmannosamine (1,6-Pr₂ManNAz), phenylboronic acid (PBA), benzoxaborole (BOB), β-galactoside α-2,3-sialyltransferase 1 (ST3Gal1), β-galactoside α-2,6-sialyltransferase 1 (ST6Gal1), *Campylobacter jejuni* β(1–4) N-acetylgalactosaminyltransferase (CgtA), and *Escherichia coli* fucosyltransferase (WbwK).

Table 3. Comparison of the quantitative analysis and imaging approaches for glycans.

Method	Target	Application	Sensitivity	Linear Range	Ref.
Optics	Sia	Quantification of Sia on PD-L1 of cell surface	-	-	[119]
	Terminal Gal, Sia	Quantification of Sia and Gal of sperm	-	-	[120]
	Integrin- α _x β ₂ /EGFR/TGF-β receptor-specific Sia	Imaging glycans on specific proteins (FRET)	-	-	[126]
	IL-36R-specific Sia	Imaging glycans on specific proteins (FRET)	-	-	[127]
	EGFR-specific Sia	Imaging glycans on specific proteins (FRET)	-	-	[129]
	EpCAM-specific Sia	Imaging glycans on specific proteins (SERS)	-	-	[130]
	Man	In situ and dynamically evaluating N-glycans in live cells (colorimetric and fluorescence)	Colorimetric method: 33 cells/mL; fluorescence method: 26 cells/mL	Colorimetric method: 100 to 1.0 × 10 ⁷ cells/mL; fluorescence method: 80–5.0 × 10 ⁷ cells/mL	[131]
	Glu	Quantitative glucose detection (SERS)	1.8 mM	0–25 mM	[136]
	Glu	Detection of glucose in urine (SERS)	-	-	[137]

Table 3. Cont.

Method	Target	Application	Sensitivity	Linear Range	Ref.
Optics	Man, Sia, GlcNAc	Quantification of multiple glycans on intact cell surfaces (SERS)	-	-	[139]
	Sia	Imaging Sia at single-cell level (SERS)	-	-	[140]
	Man, Sia, Gal, Fuc	In situ monitoring of glycans on the surface of cells in body fluids (SERS)	-	-	[142]
Electrochemistry	Sia	Highly specific and sensitive detection in serum (DPV)	10 pg/mL	10–500 pg/mL	[146]
	Man	Monitoring of glycans on living cells in response to drugs (DPV)	3000 cells/mL	$1 \times 10^4 \sim 1 \times 10^7$ cells/mL	[147]
	Sia	PSA detection (LSV)	0.2 pg/mL	0.5–200 pg/mL	[148]
	Recombinant glycoproteins	Accurate and sensitive determination (DPV)	5.3 pg/mL	0.01–50 ng/mL	[149]
	Cell-surface N-glycans	Evaluation of surface N-glycans (DPV)	10 cells	$1.0 \times 10^2 \sim 5.0 \times 10^4$ cells/mL	[150]
	Cell-surface N-glycans	Evaluation of surface N-glycans (I-t curve)	3 cells/mL	$1 \times 10^2 \sim 1 \times 10^6$ cells/mL	[151]
	AFP	Evaluating the AFP N-glycans and discriminating AFP between healthy and cancer patient's serum (EIS)	0.1 ng/L	1–100 ng/L	[152]
	Man	Monitoring of glycans on living cells (DPV)	1.5×10^3 cell/mL	$2.0 \times 10^3 \sim 2.0 \times 10^6$ cell/mL	[164]
	Man	Label-free analysis of cell-surface glycans (electrochemiluminescence)	1.2×10^3 cells/mL	$2 \times 10^3 \sim 1 \times 10^7$ cells/mL	[165]
	Man	Monitoring the dynamic variation of glycans in cancer cells (electrochemiluminescence)	100 cells/mL	$1 \times 10^2 \sim 1 \times 10^6$ cells/mL	[167]
Mass	N-glycans	Dynamically evaluating cell-surface N-glycans (electrochemiluminescence)	600 cells/mL	$1 \times 10^3 \sim 1 \times 10^7$ cells/mL	[169]
	N-glycans	Evaluation of cancer cell-surface glycans (electrochemiluminescence)	38 cells/mL	$1.0 \times 10^2 \sim 1.0 \times 10^5$ cells/mL	[170]
	MUC1-specific Sia	Quantification of MUC1-specific Sia in breast cells (LC-MS/MS)	50 pM	50 pM–10 nM	[101]
	Man, Sia, GlcNAc	Fast and in situ multiplexed glycan detection (LDI-MS)	200 cells/mL (Man)	$5 \times 10^2 \sim 2 \times 10^5$ cells/mL (Man)	[172]

Table 3. Cont.

Method	Target	Application	Sensitivity	Linear Range	Ref.
Mass	Man, Gal	Imaging glycomic alterations in cancer cells (MALDI-TOF MS)	-	-	[176]
	Sialoglycoconjugates	In situ detection of cell-surface sialoglycoconjugates (LDI-MS)	5 fmol	100 fmol~100 pmol	[178]

Epidermal growth factor receptor (EGFR), transforming growth factor- β (TGF- β), interleukin-36 receptor (IL-36R), epithelial cell adhesion molecule (EpCAM), fluorescence resonance energy transfer (FRET), surface-enhanced Raman scattering (SERS), differential pulse voltammetry (DPV), prostate-specific antigen (PSA), linear sweep voltammetry (LSV), amperometric i-t curve (I-t curve), alpha-fetoprotein (AFP), electrochemical impedance spectroscopy (EIS), liquid chromatograph mass spectrometer (LC-MS), laser desorption/ionization mass spectrometry (LDI-MS), and matrix-assisted laser desorption/ionization time-of-flight mass spectrometry (MALDI-TOF MS).

5. Conclusions

As biomolecules in the outermost layer of cell membranes, glycans play key roles in molecular recognition, signal transduction, and cellular communication. In situ imaging and quantitative analysis of glycans can help gain insight into the role of glycans in living systems and changes in disease occurrence and development. From the above examples of glycan analysis and imaging, it can be concluded that the use of optical methods to detect glycans has the advantages of high spatial resolution and good selectivity. A variety of glycan labeling techniques, including biorecognition and chemical labeling, can be used for this mode, among which chemical labeling produces lower steric resistance, thus being conducive to the visualization of glycan molecules at a smaller spatial scale. Its development trend is mainly single-cell and single-molecule glycan analysis. Electrochemical detection methods have irreplaceable advantages such as quantitative detection and high sensitivity, which are promising for medical-related diagnosis. For mass spectrometry methods, labeling agents based on lectin recognition can better match the advantage of multi-channel detection of MS. Comparatively, traditional glycan analysis methods such as biomolecular layer interferometry and microscale thermophoresis are more suitable for ex situ analysis of the recognition interactions, while more advanced methods such as SPR and AFM have the potential to achieve both glycan imaging and molecular force studies.

The next research priorities for in situ glycan sensing include (1) the limited variety of artificial/natural recognition molecules for different glycan types, and their specificity and affinity need to be further improved; (2) how to achieve spatial specificity control of metabolic and chemo-enzymatic glycan labeling techniques; (3) how to further improve the labeling efficiency; (4) the lack of standardized, comprehensive, and systematic work for in situ glycan sensing; and (5) the difficulty of dynamically tracking in situ glycan changes.

To meet these challenges, interdisciplinary collaboration between experts from different fields is essential. On the one hand, molecular simulation, structural design, and chemical and genetic modification can expand the range of labeled targets and improve their specificity, affinity, and efficiency; on the other hand, there is a need to incorporate more methods and instrumentation, such as nanomaterials, multimodal analysis, single-molecule fluorescence analysis, electrochemical analysis, high-content cell imaging, in situ mass spectrometry imaging, and so on. These will provide more technologies and support for the development of glycomics, glycochemistry, and glycobiology.

Author Contributions: Y.L.: literature review, manuscript preparation, and writing—original draft. L.W.: literature review, manuscript preparation, and writing—original draft. L.D.: review and edits. H.J.: review and edits. All authors have read and agreed to the published version of the manuscript.

Funding: We gratefully acknowledge the support from the National Natural Science Foundation of China (22274073, 21974067), Fundamental Research Funds for the Central Universities (020514380309,

021414380502, 2022300324), and the State Key Laboratory of Analytical Chemistry for Life Science (5431ZZXM2305, 5431ZZXM2204).

Institutional Review Board Statement: Not applicable.

Informed Consent Statement: Not applicable.

Data Availability Statement: Data sharing not applicable.

Conflicts of Interest: The authors declare no conflicts of interest.

References

1. Reily, C.; Stewart, T.J.; Renfrow, M.B.; Novak, J. Glycosylation in health and disease. *Nat. Rev. Nephrol.* **2019**, *15*, 346–366. [[CrossRef](#)] [[PubMed](#)]
2. Pinho, S.S.; Reis, C.A. Glycosylation in cancer: Mechanisms and clinical implications. *Nat. Rev. Cancer* **2015**, *15*, 540–555. [[CrossRef](#)] [[PubMed](#)]
3. Rudd, P.M.; Elliott, T.; Cresswell, P.; Wilson, I.A.; Dwek, R.A. Glycosylation and the immune system. *Science* **2001**, *291*, 2370–2376. [[CrossRef](#)] [[PubMed](#)]
4. Parekh, R.; Dwek, R.; Sutton, B.; Fernandes, D.; Leung, A.; Stanworth, D.; Rademacher, T.; Mizuochi, T.; Taniguchi, T.; Matsuta, K. Association of rheumatoid arthritis and primary osteoarthritis with changes in the glycosylation pattern of total serum IgG. *Nature* **1985**, *316*, 452–457. [[CrossRef](#)] [[PubMed](#)]
5. Marth, J.D.; Grewal, P.K. Mammalian glycosylation in immunity. *Nat. Rev. Immunol.* **2008**, *8*, 874–887. [[CrossRef](#)] [[PubMed](#)]
6. Goto, Y.; Uematsu, S.; Kiyono, H. Epithelial glycosylation in gut homeostasis and inflammation. *Nat. Immunol.* **2016**, *17*, 1244–1251. [[CrossRef](#)]
7. Reticker-Flynn, N.E.; Bhatia, S.N. Aberrant glycosylation promotes lung cancer metastasis through adhesion to galectins in the metastatic niche. *Cancer Discov.* **2015**, *5*, 168–181. [[CrossRef](#)]
8. Thomas, D.; Rathinavel, A.K.; Radhakrishnan, P. Altered glycosylation in cancer: A promising target for biomarkers and therapeutics. *Biochim. Biophys. Acta Rev. Cancer* **2021**, *1875*, 188464. [[CrossRef](#)]
9. Durand, G.; Seta, N. Protein glycosylation and diseases: Blood and urinary oligosaccharides as markers for diagnosis and therapeutic monitoring. *Clin. Chem.* **2000**, *46*, 795–805. [[CrossRef](#)]
10. Theodoratou, E.; Campbell, H.; Ventham, N.T.; Kolarich, D.; Pučić-Baković, M.; Zoldoš, V.; Fernandes, D.; Pemberton, I.K.; Rudan, I.; Kennedy, N.A. The role of glycosylation in IBD. *Nat. Rev. Gastroenterol. Hepatol.* **2014**, *11*, 588–600. [[CrossRef](#)]
11. Costa, A.F.; Campos, D.; Reis, C.A.; Gomes, C. Targeting glycosylation: A new road for cancer drug discovery. *Trends Cancer* **2020**, *6*, 757–766. [[CrossRef](#)] [[PubMed](#)]
12. Mereiter, S.; Balmaña, M.; Campos, D.; Gomes, J.; Reis, C.A. Glycosylation in the era of cancer-targeted therapy: Where are we heading? *Cancer Cell* **2019**, *36*, 6–16. [[CrossRef](#)] [[PubMed](#)]
13. Dotz, V.; Haselberg, R.; Shubhakar, A.; Kozak, R.P.; Falck, D.; Rombouts, Y.; Reusch, D.; Somsen, G.W.; Fernandes, D.L.; Wuhrer, M. Mass spectrometry for glycosylation analysis of biopharmaceuticals. *TrAC-Trends Anal. Chem.* **2015**, *73*, 1–9. [[CrossRef](#)]
14. Dwek, R.A.; Butters, T.D.; Platt, F.M.; Zitzmann, N. Targeting glycosylation as a therapeutic approach. *Nat. Rev. Drug Discov.* **2002**, *1*, 65–75. [[CrossRef](#)] [[PubMed](#)]
15. Weis, W.I.; Drickamer, K. Structural basis of lectin-carbohydrate recognition. *Annu. Rev. Biochem.* **1996**, *65*, 441–473. [[CrossRef](#)] [[PubMed](#)]
16. Lis, H.; Sharon, N. Lectins as molecules and as tools. *Annu. Rev. Biochem.* **1986**, *55*, 35–67. [[CrossRef](#)]
17. Kilpatrick, D.C. Animal lectins: A historical introduction and overview. *Biochim. Biophys. Acta* **2002**, *1572*, 187–197. [[CrossRef](#)]
18. Kaji, H.; Saito, H.; Yamauchi, Y.; Shinkawa, T.; Taoka, M.; Hirabayashi, J.; Kasai, K.-i.; Takahashi, N.; Isobe, T. Lectin affinity capture, isotope-coded tagging and mass spectrometry to identify N-linked glycoproteins. *Nat. Biotechnol.* **2003**, *21*, 667–672. [[CrossRef](#)]
19. Wu, D.; Li, J.; Struwe, W.B.; Robinson, C.V. Probing N-glycoprotein microheterogeneity by lectin affinity purification-mass spectrometry analysis. *Chem. Sci.* **2019**, *10*, 5146–5155. [[CrossRef](#)]
20. Regnier, F.E.; Jung, K.; Hooser, S.B.; Wilson, C.R. Glycoproteomics based on lectin affinity chromatographic selection of glycoforms. In *Lectins: Analytical Technologies*; Elsevier Science: Amsterdam, The Netherlands, 2007; pp. 193–212.
21. Safina, G. Application of surface plasmon resonance for the detection of carbohydrates, glycoconjugates, and measurement of the carbohydrate-specific interactions: A comparison with conventional analytical techniques. A critical review. *Anal. Chim. Acta* **2012**, *712*, 9–29. [[CrossRef](#)]
22. Hendrickson, O.D.; Zherdev, A.V. Analytical application of lectins. *Crit. Rev. Anal. Chem.* **2018**, *48*, 279–292. [[CrossRef](#)] [[PubMed](#)]
23. Fard, M.G.; Khabir, Z.; Reineck, P.; Cordina, N.M.; Abe, H.; Ohshima, T.; Dalal, S.; Gibson, B.C.; Packer, N.H.; Parker, L.M. Targeting cell surface glycans with lectin-coated fluorescent nanodiamonds. *Nanoscale Adv.* **2022**, *4*, 1551–1564. [[CrossRef](#)] [[PubMed](#)]
24. Gewailly, M.S.; Kassab, M.; Aboelnour, A.; Almadaly, E.A.; Noreldin, A.E. Comparative cellular localization of sugar residues in bull (*Bos taurus*) and donkey (*Equus asinus*) testes using lectin histochemistry. *Microsc. Microanal.* **2021**, *27*, 1529–1538. [[CrossRef](#)] [[PubMed](#)]

25. Nagai-Okatani, C.; Nagai, M.; Sato, T.; Kuno, A. An improved method for cell type-selective glycomic analysis of tissue sections assisted by fluorescence laser microdissection. *Int. J. Mol. Sci.* **2019**, *20*, 700. [[CrossRef](#)] [[PubMed](#)]
26. Yamamoto, T.; Sato, K.; Wakahara, S.; Mitamura, K.; Taga, A. A method for detecting tumor cells derived from colorectal cancer by targeting cell surface glycosylation with affinity capillary electrophoresis. *J. Pharm. Biomed. Anal.* **2020**, *182*, 113138. [[CrossRef](#)] [[PubMed](#)]
27. Geijtenbeek, T.B.H.; Gringhuis, S.I. C-type lectin receptors in the control of T helper cell differentiation. *Nat. Rev. Immunol.* **2016**, *16*, 433–448. [[CrossRef](#)] [[PubMed](#)]
28. Chen, C.H.; Floyd, H.; Olson, N.E.; Magaletti, D.; Li, C.; Draves, K.; Clark, E.A. Dendritic-cell-associated C-type lectin 2 (DCAL-2) alters dendritic-cell maturation and cytokine production. *Blood* **2006**, *107*, 1459–1467. [[CrossRef](#)]
29. Tommasone, S.; Allabush, F.; Tagger, Y.K.; Norman, J.; Köpf, M.; Tucker, J.H.R.; Mendes, P.M. The challenges of glycan recognition with natural and artificial receptors. *Chem. Soc. Rev.* **2019**, *48*, 5488–5505. [[CrossRef](#)]
30. Beckwith, D.M.; FitzGerald, F.G.; Rodriguez Benavente, M.C.; Mercer, E.R.; Ludwig, A.K.; Michalak, M.; Kaltner, H.; Kopitz, J.; Gabius, H.J.; Cudic, M. Calorimetric analysis of the interplay between synthetic Tn antigen-presenting MUC1 glycopeptides and human macrophage galactose-type lectin. *Biochemistry* **2021**, *60*, 547–558. [[CrossRef](#)]
31. Li, P.J.; Anwar, M.T.; Fan, C.Y.; Juang, D.S.; Lin, H.Y.; Chang, T.C.; Kawade, S.K.; Chen, H.J.; Chen, Y.J.; Tan, K.T.; et al. Fluorescence “turn-on” lectin sensors fabricated by ligand-assisted labeling probes for detecting protein–glycoprotein interactions. *Biomacromolecules* **2020**, *21*, 815–824. [[CrossRef](#)]
32. Xie, Y.X.; Sheng, Y.; Li, Q.Y.; Ju, S.; Reyes, J.; Lebrilla, C.B. Determination of the glycoprotein specificity of lectins on cell membranes through oxidative proteomics. *Chem. Sci.* **2020**, *11*, 9501–9512. [[CrossRef](#)] [[PubMed](#)]
33. Donahue, T.C.; Zong, G.H.; O’Brien, N.A.; Ou, C.; Gildersleeve, J.C.; Wang, L.X. Synthesis and immunological study of N-glycan-bacteriophage Q β conjugates reveal dominant antibody responses to the conserved chitobiose core. *Bioconjugate Chem.* **2022**, *33*, 1350–1362. [[CrossRef](#)] [[PubMed](#)]
34. Koprowski, H.; Stepiewski, Z.; Mitchell, K.; Herlyn, M.; Herlyn, D.; Fuhrer, P. Colorectal carcinoma antigens detected by hybridoma antibodies. *Somat. Cell Mol. Genet.* **1979**, *5*, 957–971. [[CrossRef](#)] [[PubMed](#)]
35. Li, B.; Li, Y.X.; Li, C.C.; Yang, J.H.; Liu, D.L.; Wang, H.B.; Xu, R.; Zhang, Y.; Wei, Q. An ultrasensitive split-type electrochemical immunosensor based on controlled-release strategy for detection of CA19-9. *Biosens. Bioelectron.* **2023**, *227*, 115180. [[CrossRef](#)] [[PubMed](#)]
36. Kim, J.; Bamlet, W.R.; Oberg, A.L.; Chaffee, K.G.; Donahue, G.; Cao, X.J.; Chari, S.; Garcia, B.A.; Petersen, G.M.; Zaret, K.S. Detection of early pancreatic ductal adenocarcinoma with thrombospondin-2 and CA19-9 blood markers. *Sci. Transl. Med.* **2017**, *9*, eaah5583. [[CrossRef](#)]
37. Partyka, K.; Maupin, K.A.; Brand, R.E.; Haab, B.B. Diverse monoclonal antibodies against the CA 19-9 antigen show variation in binding specificity with consequences for clinical interpretation. *Proteomics* **2012**, *12*, 2212–2220. [[CrossRef](#)]
38. Thakur, M.L.; Marcus, C.S.; Henneman, P.; Butler, J.; Sinow, R.; Diggles, L.; Minami, C.; Mason, G.; Klein, S.; Rhodes, B. Imaging inflammatory diseases with neutrophil-specific technetium-99m-labeled monoclonal antibody anti-SSEA-1. *J. Nucl. Med.* **1996**, *37*, 1789–1795.
39. Briard, J.G.; Jiang, H.; Moremen, K.W.; Macauley, M.S.; Wu, P. Cell-based glycan arrays for probing glycan–glycan binding protein interactions. *Nat. Commun.* **2018**, *9*, 880. [[CrossRef](#)]
40. Kurtenkov, O.; Innos, K.; Sergejev, B.; Klaamas, K. The Thomsen-Friedenreich Antigen-Specific Antibody Signatures in Patients with Breast Cancer. *BioMed Res. Int.* **2018**, *2018*, 9579828. [[CrossRef](#)]
41. Kreft, L.; Schepers, A.; Hils, M.; Swiontek, K.; Flatley, A.; Janowski, R.; Mirzaei, M.K.; Dittmar, M.; Charkrapani, N.; Desai, M.S.; et al. A novel monoclonal IgG1 antibody specific for Galactose- α -1,3-galactose questions α -Gal epitope expression by bacteria. *Front. Immunol.* **2022**, *13*, 958952. [[CrossRef](#)]
42. Kappler, K.; Hennet, T. Emergence and significance of carbohydrate-specific antibodies. *Genes Immun.* **2020**, *21*, 224–239. [[CrossRef](#)] [[PubMed](#)]
43. Butler, D.L.; Imberti, L.; Quaresima, V.; Fiorini, C.; Gildersleeve, J.C.; NIAID COVID-19 Consortium. Abnormal antibodies to self-carbohydrates in SARS-CoV-2-infected patients. *PNAS Nexus* **2022**, *1*, pgac062. [[CrossRef](#)] [[PubMed](#)]
44. Tuerk, C.; Gold, L. Systematic evolution of ligands by exponential enrichment: RNA ligands to bacteriophage T4 DNA polymerase. *Science* **1990**, *249*, 505–510. [[CrossRef](#)]
45. Zhao, L.H.; Qi, X.Y.; Yan, X.C.; Huang, Y.F.; Liang, X.G.; Zhang, L.; Wang, S.; Tan, W.H. Engineering aptamer with enhanced affinity by triple helix-based terminal fixation. *J. Am. Chem. Soc.* **2019**, *141*, 17493–17497. [[CrossRef](#)] [[PubMed](#)]
46. Kawakami, J.; Kawase, Y.; Sugimoto, N. In vitro selection of aptamers that recognize a monosaccharide. *Anal. Chim. Acta* **1998**, *365*, 95–100. [[CrossRef](#)]
47. Mehedi Masud, M.; Kuwahara, M.; Ozaki, H.; Sawai, H. Sialyllactose-binding modified DNA aptamer bearing additional functionality by SELEX. *Bioorg. Med. Chem.* **2004**, *12*, 1111–1120. [[CrossRef](#)]
48. Chen, J.; Chen, X.; Zhang, Y.; Wang, X.; Zhou, N. Screening of a Sialyllactose-Specific Aptamer and Engineering a Pair of Recognition Elements with Unique Fluorescent Characteristics for Sensitive Detection of Sialyllactose. *J. Agric. Food Chem.* **2023**, *71*, 2628–2636. [[CrossRef](#)]
49. Jeong, S.; Eom, T.Y.; Kim, S.J.; Lee, S.W.; Yu, J. In vitro selection of the RNA aptamer against the Sialyl Lewis X and its inhibition of the cell adhesion. *Biochem. Biophys. Res. Commun.* **2001**, *281*, 237–243. [[CrossRef](#)]

50. Ma, Y.; Li, X.; Li, W.; Liu, Z. Glycan-imprinted magnetic nanoparticle-based SELEX for efficient screening of glycoprotein-binding aptamers. *ACS Appl. Mater. Interfaces* **2018**, *10*, 40918–40926. [[CrossRef](#)]
51. Li, W.; Ma, Y.; Guo, Z.; Xing, R.; Liu, Z. Efficient screening of glycan-specific aptamers using a glycosylated peptide as a scaffold. *Anal. Chem.* **2021**, *93*, 956–963. [[CrossRef](#)]
52. Sminia, T.J.; Zuilhof, H.; Wennekes, T. Getting a grip on glycans: A current overview of the metabolic oligosaccharide engineering toolbox. *Carbohydr. Res.* **2016**, *435*, 121–141. [[CrossRef](#)] [[PubMed](#)]
53. Cheng, B.; Tang, Q.; Zhang, C.; Chen, X. Glycan labeling and analysis in cells and in vivo. *Annu. Rev. Anal. Chem.* **2021**, *14*, 363–387. [[CrossRef](#)] [[PubMed](#)]
54. Bertozzi, C.R.; Kiessling, L.L. Chemical glycobiology. *Science* **2001**, *291*, 2357–2364. [[CrossRef](#)] [[PubMed](#)]
55. Dube, D.H.; Bertozzi, C.R. Metabolic oligosaccharide engineering as a tool for glycobiology. *Curr. Opin. Chem. Biol.* **2003**, *7*, 616–625. [[CrossRef](#)] [[PubMed](#)]
56. Goon, S.; Bertozzi, C.R. Metabolic substrate engineering as a tool for glycobiology. *J. Carbohydr. Chem.* **2002**, *21*, 943–977. [[CrossRef](#)]
57. Kizuka, Y.; Funayama, S.; Shogomori, H.; Nakano, M.; Nakajima, K.; Oka, R.; Kitazume, S.; Yamaguchi, Y.; Sano, M.; Korekane, H.; et al. High-sensitivity and low-toxicity fucose probe for glycan imaging and biomarker discovery. *Cell Chem. Biol.* **2016**, *23*, 782–792. [[CrossRef](#)]
58. Hao, Y.; Fan, X.; Shi, Y.; Zhang, C.; Sun, D.-E.; Qin, K.; Qin, W.; Zhou, W.; Chen, X. Next-generation unnatural monosaccharides reveal that ESRRB O-GlcNAcylation regulates pluripotency of mouse embryonic stem cells. *Nat. Commun.* **2019**, *10*, 4065. [[CrossRef](#)]
59. Chen, D.X.; Lin, Y.Y.; Li, A.; Luo, X.J.; Yang, C.Y.; Gao, J.H.; Lin, H.Y. Bio-orthogonal metabolic fluorine labeling enables deep-tissue visualization of tumor cells in vivo by ¹⁹F magnetic resonance imaging. *Anal. Chem.* **2022**, *94*, 16614–16621. [[CrossRef](#)]
60. Wang, Y.J.; Li, L.; Yu, J.; Hu, H.Y.; Liu, Z.X.; Jiang, W.J.; Xu, W.; Guo, X.P.; Wang, F.S.; Sheng, J.Z. Imaging of Escherichia coli K5 and glycosaminoglycan precursors via targeted metabolic labeling of capsular polysaccharides in bacteria. *Sci. Adv.* **2023**, *9*, eade4770. [[CrossRef](#)]
61. Parle, D.R.; Bulat, F.; Fouad, S.; Zecchini, H.; Brindle, K.M.; Neves, A.A.; Leeper, F.J. Metabolic glycan labeling of cancer cells using variably acetylated monosaccharides. *Bioconjug. Chem.* **2022**, *33*, 1467–1473. [[CrossRef](#)]
62. Qin, W.; Qin, K.; Fan, X.; Peng, L.; Hong, W.; Zhu, Y.; Lv, P.; Du, Y.; Huang, R.; Han, M.; et al. Artificial cysteine S-glycosylation induced by per-O-acetylated unnatural monosaccharides during metabolic glycan labeling. *Angew. Chem. Int. Ed.* **2018**, *57*, 1817–1820. [[CrossRef](#)] [[PubMed](#)]
63. Qin, K.; Zhang, H.; Zhao, Z.; Chen, X. Protein S-glyco-modification through an elimination–addition mechanism. *J. Am. Chem. Soc.* **2020**, *142*, 9382–9388. [[CrossRef](#)] [[PubMed](#)]
64. Sun, J.Y.; Huang, Z.M.; Du, Y.F.; Lv, P.; Fan, X.Q.; Dai, P.; Chen, X. Metabolic glycan labeling in primary neurons enabled by unnatural sugars with no S-glyco-modification. *ACS Chem. Biol.* **2023**, *18*, 1416–1424. [[CrossRef](#)] [[PubMed](#)]
65. Lopez Aguilar, A.; Briard, J.G.; Yang, L.; Ovryn, B.; Macauley, M.S.; Wu, P. Tools for studying glycans: Recent advances in chemoenzymatic glycan labeling. *ACS Chem. Biol.* **2017**, *12*, 611–621. [[CrossRef](#)] [[PubMed](#)]
66. Yan, Y.R.; Mo, T.; Huang, W.Q.; Xu, X.P.; Tian, W.S.; Wang, Y.X.; Song, Y.L.; Li, J.; Shi, S.; Liu, X.; et al. Glycosylation of aromatic glycosides by a promiscuous glycosyltransferase UGT71BD1 from *Cistanche tubulosa*. *J. Nat. Prod.* **2022**, *85*, 1826–1836. [[CrossRef](#)] [[PubMed](#)]
67. Guo, B.D.; Hou, X.D.; Zhang, Y.; Deng, Z.W.; Ping, Q.; Fu, K.; Yuan, Z.B.; Rao, Y.J. Highly efficient production of rebaudioside D enabled by structure-guided engineering of bacterial glycosyltransferase YojK. *Front. Bioeng. Biotechnol.* **2022**, *10*, 985826. [[CrossRef](#)]
68. Zhong, R.Q.; Phillips, D.R.; Adams, E.R.; Ye, Z.H. An Arabidopsis family GT106 glycosyltransferase is essential for xylan biosynthesis and secondary wall deposition. *Planta* **2023**, *257*, 43. [[CrossRef](#)]
69. Tan, Y.M.; Zhang, X.; Feng, Y.; Yang, G.Y. Directed evolution of glycosyltransferases by a single-cell ultrahigh-throughput FACS-based screening method. *Methods Mol. Biol.* **2022**, *2461*, 211–224.
70. Deng, J.Q.; Lu, Z.; Liu, J.; Zhao, Y.; Hou, X.B.; Guo, X.P.; Jiang, W.J.; Wang, F.S.; Sheng, J.Z. Heparosan oligosaccharide synthesis using engineered single-function glycosyltransferases. *Catal. Sci. Technol.* **2022**, *12*, 3793–3803. [[CrossRef](#)]
71. Cid, E.; Yamamoto, M.; Yamamoto, F. Mixed-up sugars: Glycosyltransferase cross-reactivity in cancerous tissues and their therapeutic targeting. *ChemBioChem* **2022**, *23*, e202100460. [[CrossRef](#)]
72. Hirata, T.; Harada, Y.; Hirosawa, K.M.; Tokoro, Y.; Suzuki, K.G.; Kizuka, Y. N-acetylglucosaminyltransferase-V (GnT-V)-enriched small extracellular vesicles mediate N-glycan remodeling in recipient cells. *iScience* **2023**, *26*, 105747. [[CrossRef](#)] [[PubMed](#)]
73. Büll, C.; Nason, R.; Sun, L.; Van Coillie, J.; Madriz Sørensen, D.; Moons, S.J.; Yang, Z.; Arbitman, S.; Fernandes, S.M.; Furukawa, S.; et al. Probing the binding specificities of human Siglecs by cell-based glycan arrays. *Proc. Natl. Acad. Sci. USA* **2021**, *118*, e2026102118. [[CrossRef](#)] [[PubMed](#)]
74. Babulic, J.L.; Capicciotti, C.J. Exo-enzymatic cell-surface glycan labeling for capturing glycan–protein interactions through photo-cross-linking. *Bioconjug. Chem.* **2022**, *33*, 773–780. [[CrossRef](#)] [[PubMed](#)]
75. Wu, Q.; Ye, J.; Chao, Y.; Dong, S.; Niu, M.; Wang, Y.; Liu, Z.; Chen, W.; Ge, N.; Lu, S.; et al. Chemoenzymatic labeling pathogens containing terminal N-acetylneuraminic acid- α (2-3)-galactose glycans. *ACS Infect. Dis.* **2022**, *8*, 657–664. [[CrossRef](#)]

76. Li, Q.; Li, Z.; Duan, X.; Yi, W. A tandem enzymatic approach for detecting and imaging tumor-associated Thomsen-Friedenreich antigen disaccharide. *J. Am. Chem. Soc.* **2014**, *136*, 12536–12539. [[CrossRef](#)]
77. Whittaker, J.W. Free radical catalysis by galactose oxidase. *Chem. Rev.* **2003**, *103*, 2347–2364. [[CrossRef](#)]
78. Rannes, J.B.; Ioannou, A.; Willies, S.C.; Grogan, G.; Behrens, C.; Flitsch, S.L.; Turner, N.J. Glycoprotein labeling using engineered variants of galactose oxidase obtained by directed evolution. *J. Am. Chem. Soc.* **2011**, *133*, 8436–8439. [[CrossRef](#)]
79. Matthey, A.P.; Birmingham, W.R.; Both, P.; Kress, N.; Huang, K.; van Munster, J.M.; Bulmer, G.S.; Parmeggiani, F.; Voglmeir, J.; Martinez, J.E.R.; et al. Selective oxidation of N-glycolylneuraminic acid using an engineered galactose oxidase variant. *ACS Catal.* **2019**, *9*, 8208–8212. [[CrossRef](#)]
80. Ramya, T.N.C.; Weerapana, E.; Cravatt, B.F.; Paulson, J.C. Glycoproteomics enabled by tagging sialic acid- or galactose-terminated glycans. *Glycobiology* **2013**, *23*, 211–221. [[CrossRef](#)]
81. Han, E.; Ding, L.; Qian, R.C.; Bao, L.; Ju, H.X. Sensitive chemiluminescent imaging for chemoselective analysis of glycan expression on living cells using a multifunctional nanoprobe. *Anal. Chem.* **2012**, *84*, 1452–1458. [[CrossRef](#)]
82. Zhang, P.W.; Li, Y.R.; Yu, X.F.; Ju, H.X.; Ding, L. Switchable enzymatic accessibility for precision cell-selective surface glycan remodeling. *Chem. Eur. J.* **2019**, *25*, 10505–10510. [[CrossRef](#)]
83. Tao, J.; Yu, X.F.; Guo, Y.N.; Wang, G.Y.; Ju, H.X.; Ding, L. Proximity enzymatic glyco-remodeling enables direct and highly efficient lipid raft imaging on live cells. *Anal. Chem.* **2020**, *92*, 7232–7239. [[CrossRef](#)] [[PubMed](#)]
84. Yu, X.F.; Shi, H.F.; Li, Y.R.; Guo, Y.N.; Zhang, P.W.; Wang, G.Y.; Li, L.; Chen, X.; Ding, L.; Ju, H.X. Thermally triggered, cell-specific enzymatic glyco-editing: In situ regulation of lectin recognition and immune response on target cells. *ACS Appl. Mater. Interfaces* **2020**, *12*, 54387–54398. [[CrossRef](#)] [[PubMed](#)]
85. Li, S.Q.; Mao, A.W.; Huo, F.; Wang, X.J.; Guo, Y.N.; Liu, L.; Yan, C.; Ding, L.; Ju, H.X. A localized glyco-editing probe for revelation of protein-specific glycan function. *Mater. Today* **2021**, *49*, 85–96. [[CrossRef](#)]
86. Guo, Y.N.; Tao, J.; Li, Y.R.; Feng, Y.M.; Ju, H.X.; Wang, Z.F.; Ding, L. Quantitative localized analysis reveals distinct exosomal protein-specific glycosignatures: Implications in cancer cell subtyping, exosome biogenesis, and function. *J. Am. Chem. Soc.* **2020**, *142*, 7404–7412. [[CrossRef](#)] [[PubMed](#)]
87. Mao, A.W.; Zhang, Y.; Wang, G.Y.; Zhong, T.; Chen, X.Y.; Wang, H.Q.; Xie, R.; Wang, X.J.; Ding, L.; Ju, H.X. Aglycone sterics-selective enzymatic glycan remodeling. *iScience* **2022**, *25*, 104578. [[CrossRef](#)]
88. Otsuka, H.; Uchimura, E.; Koshino, H.; Okano, T.; Kataoka, K. Anomalous binding profile of phenylboronic acid with N-acetylneuraminic acid (Neu5Ac) in aqueous solution with varying pH. *J. Am. Chem. Soc.* **2003**, *125*, 3493–3502. [[CrossRef](#)]
89. Matsumoto, A.; Sato, N.; Kataoka, K.; Miyahara, Y. Noninvasive sialic acid detection at cell membrane by using phenylboronic acid modified self-assembled monolayer gold electrode. *J. Am. Chem. Soc.* **2009**, *131*, 12022–12023. [[CrossRef](#)]
90. Li, T.; Liu, Y. Self-assembled nanorods of phenylboronic acid functionalized pyrene for in situ two-photon imaging of cell surface sialic acids and photodynamic therapy. *Anal. Chem.* **2021**, *93*, 7029–7036. [[CrossRef](#)]
91. Miyazaki, T.; Khan, T.; Tachihara, Y.; Itoh, M.; Miyazawa, T.; Suganami, T.; Miyahara, Y.; Cabral, H.; Matsumoto, A. Boronic acid ligands can target multiple subpopulations of pancreatic cancer stem cells via pH-dependent glycan-terminal sialic acid recognition. *ACS Appl. Bio. Mater.* **2021**, *4*, 6647–6651. [[CrossRef](#)]
92. Qualls, M.L.; Hagedorn, H.; Lou, J.; Mattern-Schain, S.I.; Zhang, X.Y.; Mountain, D.J.; Best, M.D. Bis-boronic acid liposomes for carbohydrate recognition and cellular delivery. *ChemBioChem* **2022**, *23*, e202200402. [[CrossRef](#)] [[PubMed](#)]
93. Wulff, G.; Lauer, M.; Böhnke, H. Rapid proton transfer as cause of an unusually large neighboring group effect. *Angew. Chem. Int. Ed.* **1984**, *23*, 741–742. [[CrossRef](#)]
94. Ye, S.; Han, T.; Cheng, M.; Dong, L. Wulff-type boronic acid-functionalized quantum dots for rapid and sensitive detection of Gram-negative bacteria. *Sens. Actuators B Chem.* **2022**, *356*, 131332. [[CrossRef](#)]
95. Dowlut, M.; Hall, D.G. An improved class of sugar-binding boronic acids, soluble and capable of complexing glycosides in neutral water. *J. Am. Chem. Soc.* **2006**, *128*, 4226–4227. [[CrossRef](#)] [[PubMed](#)]
96. Sorensen, M.D.; Martins, R.; Hindsgaul, O. Assessing the terminal glycosylation of a glycoprotein by the naked eye. *Angew. Chem. Int. Ed.* **2007**, *46*, 2403–2407. [[CrossRef](#)] [[PubMed](#)]
97. Lindstedt, G. Periodate oxidation of sugars in neutral phosphate buffer. *Nature* **1945**, *156*, 448–449. [[CrossRef](#)]
98. Zeng, Y.; Ramya, T.; Dirksen, A.; Dawson, P.E.; Paulson, J.C. High-efficiency labeling of sialylated glycoproteins on living cells. *Nat. Methods* **2009**, *6*, 207–209. [[CrossRef](#)]
99. Chen, B.B.; Wang, X.Y.; Qian, R.C. Rolling “wool-balls”: Rapid live-cell mapping of membrane sialic acids via poly-p-benzoquinone/ethylenediamine nanoclusters. *Chem. Commun.* **2019**, *55*, 9681–9684. [[CrossRef](#)]
100. Yang, Y.Q.; Qian, X.P.; Zhang, L.H.; Miao, W.J.; Ming, D.M.; Jiang, L.; Huang, H. Enhanced imaging of glycan expressing cancer cells using poly (glycidyl methacrylate)-grafted silica nanospheres labeled with quantum dots. *Anal. Chim. Acta* **2020**, *1095*, 138–145. [[CrossRef](#)]
101. Liu, L.; Chen, X.Y.; Sun, B. Construction of a recyclable DNAzyme motor for MUC1-specific glycoform in situ quantification. *Anal. Chem.* **2022**, *94*, 13745–13752. [[CrossRef](#)]
102. Fernandez-Poza, S.; Padros, A.; Thompson, R.; Butler, L.; Islam, M.; Mosely, J.A.; Scrivens, J.H.; Rehman, M.F.; Akram, M.S. Tailor-Made Recombinant Prokaryotic Lectins for Characterisation of Glycoproteins. *Anal. Chim. Acta* **2021**, *1155*, 338352. [[CrossRef](#)] [[PubMed](#)]

103. Tamura, T.; Omura, Y.; Kotera, K.; Ito, R.; Ohno, S.; Manabe, N.; Yamaguchi, Y.; Tamura, J. Synthesis of the Matriglycan Hexasaccharide, -3xyl α 1-3glca β 1-Trimer and Its Interaction with Laminin. *Org. Biomol. Chem.* **2022**, *20*, 8489–8500. [[CrossRef](#)] [[PubMed](#)]
104. Lim, B.; Kydd, L.; Jaworski, J. A Peptide-Lectin Fusion Strategy for Developing a Glycan Probe for Use in Various Assay Formats. *Chemosensors* **2019**, *7*, 55. [[CrossRef](#)] [[PubMed](#)]
105. Kelly, S.; Hansen, S.B.; RübSam, H.; Saake, P.; Pedersen, E.B.; Gysel, K.; Madland, E.; Wu, S.L.; Wawra, S.; Reid, D.; et al. A Glycan Receptor Kinase Facilitates Intracellular Accommodation of Arbuscular Mycorrhiza and Symbiotic Rhizobia in the Legume *Lotus japonicus*. *PLoS Biol.* **2023**, *21*, e3002127. [[CrossRef](#)] [[PubMed](#)]
106. Sáez, F.J.; Madrid, J.F.; Cardoso, S.; Gómez, L.; Hernández, F. Glycoconjugates of the Urodele Amphibian Testis Shown by Lectin Cytochemical Methods. *Microsc. Res. Tech.* **2004**, *64*, 63–76. [[CrossRef](#)] [[PubMed](#)]
107. Yu, H.J.; Zhu, M.Z.; Qiu, Y.N.; Zhong, Y.G.; Yan, H.; Wang, Q.; Bian, H.J.; Li, Z. Analysis of Glycan-Related Genes Expression and Glycan Profiles in Mice with Liver Fibrosis. *J. Proteome Res.* **2012**, *11*, 5277–5285. [[CrossRef](#)] [[PubMed](#)]
108. Hirakawa, T.; Nasu, K.; Kai, K.; Aoyagi, Y.; Ishii, T.; Uemura, T.; Yano, M.; Narahara, H. Wisteria Floribunda Agglutinin-Binding Glycan Expression Is Decreased in Endometriomata. *Reprod. Biol. Endocrinol.* **2014**, *12*, 100. [[CrossRef](#)]
109. Jones, C.J.P.; Wilsher, S.; Russo, G.; Aplin, J.D. Lectin Histochemistry Reveals Two Cytotrophoblast Differentiation Pathways During Placental Development in the Feline (*Felis catus*). *Placenta* **2023**, *134*, 30–38. [[CrossRef](#)]
110. Duk, M.; Lisowska, E.; Wu, J.H.; Wu, A.M. The biotin/avidin-mediated microtiter plate lectin assay with the use of chemically modified glycoprotein ligand. *Anal. Biochem.* **1994**, *221*, 266–272. [[CrossRef](#)]
111. Mislovičová, D.; Katrlík, J.; Paulovičová, E.; Gemeiner, P.; Tkac, J. Comparison of three distinct ELLA protocols for determination of apparent affinity constants between Con A and glycoproteins. *Colloids Surf. B* **2012**, *94*, 163–169. [[CrossRef](#)]
112. Han, C.W.; Dong, T.B.; Wang, P.C.; Zhou, F.M. Microfluidically partitioned dual channels for accurate background subtraction in cellular binding studies by surface plasmon resonance microscopy. *Anal. Chem.* **2022**, *94*, 17303–17311. [[CrossRef](#)] [[PubMed](#)]
113. Dong, T.B.; Han, C.W.; Liu, X.; Wang, Z.C.; Wang, Y.H.; Kang, Q.; Wang, P.C.; Zhou, F.M. Live cells versus fixated cells: Kinetic measurements of biomolecular interactions with the ligand tracer method and surface plasmon resonance microscopy. *Mol. Pharm.* **2023**, *20*, 2094–2104. [[CrossRef](#)] [[PubMed](#)]
114. Luo, Z.W.; Wang, Y.M.; Xu, Y.; Wang, X.; Huang, Z.J.; Chen, J.M.; Li, Y.X.; Duan, Y.X. Ultrasensitive U-shaped fiber optic LSPR cytosensing for label-free and in situ evaluation of cell surface N-glycan expression. *Sens. Actuators B Chem.* **2019**, *284*, 582–588. [[CrossRef](#)]
115. Koehler, M.; Aravamudhan, P.; Guzman-Cardozo, C.; Dumitru, A.C.; Yang, J.; Gargiulo, S.; Soumillion, P.; Dermody, T.S.; Alsteens, D. Glycan-mediated enhancement of reovirus receptor binding. *Nat. Commun.* **2019**, *10*, 4460. [[CrossRef](#)]
116. Koehler, M.; Delguste, M.; Sieben, C.; Gillet, L.; Alsteens, D. Initial step of virus entry: Virion binding to cell-surface glycans. *Annu. Rev. Virol.* **2020**, *7*, 143–165. [[CrossRef](#)]
117. Petitjean, S.J.L.; Chen, W.; Koehler, M.; Jimmidi, R.; Yang, J.; Mohammed, D.; Juniku, B.; Stanifer, M.L.; Boulant, S.; Vincent, S.P. Multivalent 9-O-Acetylated-sialic acid glycoclusters as potent inhibitors for SARS-CoV-2 infection. *Nat. Commun.* **2022**, *13*, 2564. [[CrossRef](#)]
118. Osawa, S.; Matsumoto, A.; Maejima, Y.; Suzuki, T.; Miyahara, Y.; Otsuka, H. Direct observation of cell surface sialylation by atomic force microscopy employing boronic acid–sialic acid reversible interaction. *Anal. Chem.* **2020**, *92*, 11714–11720. [[CrossRef](#)]
119. Fu, Y.; Qian, H.; Zhou, X.; Wu, Y.; Song, L.; Chen, K.; Bai, D.; Yang, Y.; Li, J.; Xie, G. Proximity ligation assay mediated rolling circle amplification strategy for in situ amplified imaging of glycosylated PD-L1. *Anal. Bioanal. Chem.* **2021**, *413*, 6929–6939. [[CrossRef](#)]
120. Xu, L.; Zhong, T.; Zhao, W.; Yao, B.; Ding, L.; Ju, H. Chemoselective labeling-based spermatozoa glycan imaging reveals abnormal glycosylation in oligoasthenospermia. *Chin. Chem. Lett.* **2023**, *34*, 108760. [[CrossRef](#)]
121. Elgavish, S.; Shaanan, B. Lectin-carbohydrate interactions: Different folds, common recognition principles. *Trends Biochem. Sci.* **1997**, *22*, 462–467. [[CrossRef](#)]
122. Hirabayashi, J.; Yamada, M.; Kuno, A.; Tateno, H. Lectin microarrays: Concept, principle and applications. *Chem. Soc. Rev.* **2013**, *42*, 4443–4458. [[CrossRef](#)] [[PubMed](#)]
123. Hsu, K.L.; Pilobello, K.T.; Mahal, L.K. Analyzing the dynamic bacterial glycome with a lectin microarray approach. *Nat. Chem. Biol.* **2006**, *2*, 153–157. [[CrossRef](#)] [[PubMed](#)]
124. Pilobello, K.T.; Slawek, D.E.; Mahal, L.K. A ratiometric lectin microarray approach to analysis of the dynamic mammalian glycome. *Proc. Natl. Acad. Sci. USA* **2007**, *104*, 11534–11539. [[CrossRef](#)] [[PubMed](#)]
125. Feng, Y.M.; Guo, Y.N.; Li, Y.R.; Tao, J.; Ding, L.; Wu, J.; Ju, H.X. Lectin-mediated in situ rolling circle amplification on exosomes for probing cancer-related glycan pattern. *Anal. Chim. Acta* **2018**, *1039*, 108–115. [[CrossRef](#)] [[PubMed](#)]
126. Lin, W.; Du, Y.F.; Zhu, Y.T.; Chen, X. A cis-membrane FRET-based method for protein-specific imaging of cell-surface glycans. *J. Am. Chem. Soc.* **2014**, *136*, 679–687. [[CrossRef](#)]
127. Li, N.; Zhang, W.; Lin, L.; Shah, S.N.A.; Li, Y.; Lin, J.M. Nongenetically encoded and erasable imaging strategy for receptor-specific glycans on live cells. *Anal. Chem.* **2019**, *91*, 2600–2604. [[CrossRef](#)]
128. Belardi, B.; de la Zerda, A.; Spiciarich, D.R.; Maund, S.L.; Peehl, D.M.; Bertozzi, C.R. Imaging the glycosylation state of cell surface glycoproteins by two-photon fluorescence lifetime imaging microscopy. *Angew. Chem. Int. Ed.* **2013**, *52*, 14045–14049. [[CrossRef](#)]
129. Haga, Y.; Ishii, K.; Hibino, K.; Sako, Y.; Ito, Y.; Taniguchi, N.; Suzuki, T. Visualizing specific protein glycoforms by transmembrane fluorescence resonance energy transfer. *Nat. Commun.* **2012**, *3*, 907. [[CrossRef](#)]

130. Chen, Y.; Ding, L.; Song, W.; Yang, M.; Ju, H.X. Liberation of protein-specific glycosylation information for glycan analysis by exonuclease III-aided recycling hybridization. *Anal. Chem.* **2016**, *88*, 2923–2928. [[CrossRef](#)]
131. Liang, L.L.; Lan, F.F.; Li, L.; Ge, S.; Yu, J.H.; Ren, N.; Liu, H.Y.; Yan, M. Paper analytical devices for dynamic evaluation of cell surface N-glycan expression via a bimodal biosensor based on multibranching hybridization chain reaction amplification. *Biosens. Bioelectron.* **2016**, *86*, 756–763. [[CrossRef](#)]
132. Swierczewska, M.; Liu, G.; Lee, S.; Chen, X. High-sensitivity nanosensors for biomarker detection. *Chem. Soc. Rev.* **2012**, *41*, 2641–2655. [[CrossRef](#)] [[PubMed](#)]
133. Reguera, J.; Langer, J.; Jimenez de Aberasturi, D.; Liz-Marzan, L.M. Anisotropic metal nanoparticles for surface enhanced Raman scattering. *Chem. Soc. Rev.* **2017**, *46*, 3866–3885. [[CrossRef](#)] [[PubMed](#)]
134. Wang, Z.Y.; Zong, S.F.; Wu, L.; Zhu, D.; Cui, Y.P. SERS-activated platforms for immunoassay: Probes, encoding methods, and applications. *Chem. Rev.* **2017**, *117*, 7910–7963. [[CrossRef](#)] [[PubMed](#)]
135. Vangala, K.; Yanney, M.; Hsiao, C.T.; Wu, W.W.; Shen, R.F.; Zou, S.; Sygula, A.; Zhang, D. Sensitive carbohydrate detection using surface enhanced Raman tagging. *Anal. Chem.* **2010**, *82*, 10164–10171. [[CrossRef](#)] [[PubMed](#)]
136. Shafer-Peltier, K.E.; Haynes, C.L.; Glucksberg, M.R.; Van Duyne, R.P. Toward a glucose biosensor based on surface-enhanced Raman scattering. *J. Am. Chem. Soc.* **2003**, *125*, 588–593. [[CrossRef](#)]
137. Sun, D.; Qi, G.H.; Xu, S.P.; Xu, W.Q. Construction of highly sensitive surface-enhanced Raman scattering (SERS) nanosensor aimed for the testing of glucose in urine. *RSC Adv.* **2016**, *6*, 53800–53803. [[CrossRef](#)]
138. Sun, F.; Bai, T.; Zhang, L.; Ella-Menye, J.R.; Liu, S.J.; Nowinski, A.K.; Jiang, S.Y.; Yu, Q.M. Sensitive and fast detection of fructose in complex media via symmetry breaking and signal amplification using surface-enhanced Raman spectroscopy. *Anal. Chem.* **2014**, *86*, 2387–2394. [[CrossRef](#)]
139. Chen, Y.L.; Ding, L.; Xu, J.Q.; Song, W.Y.; Yang, M.; Hu, J.J.; Ju, H.X. Micro-competition system for Raman quantification of multiple glycans on intact cell surface. *Chem. Sci.* **2015**, *6*, 3769–3774. [[CrossRef](#)]
140. Di, H.; Liu, H.; Li, M.; Li, J.; Liu, D. High-precision profiling of sialic acid expression in cancer cells and tissues using background-free surface-enhanced Raman scattering tags. *Anal. Chem.* **2017**, *89*, 5874–5881. [[CrossRef](#)]
141. Ye, J.; Chen, Y.; Liu, Z. A boronate affinity sandwich assay: An appealing alternative to immunoassays for the determination of glycoproteins. *Angew. Chem. Int. Ed.* **2014**, *53*, 10386–10389. [[CrossRef](#)]
142. Cordina, N.M.; Zhang, W.; Packer, N.H.; Wang, Y. Rapid and sensitive glycan targeting by lectin-SERS assay. *Mol. Omics* **2020**, *16*, 339–344. [[CrossRef](#)] [[PubMed](#)]
143. Miao, X.R.; Wen, S.P.; Su, Y.; Fu, J.J.; Luo, X.J.; Wu, P.; Cai, C.X.; Jelinek, R.; Jiang, L.P.; Zhu, J.J. Graphene quantum dots wrapped gold nanoparticles with integrated enhancement mechanisms as sensitive and homogeneous substrates for surface-enhanced Raman spectroscopy. *Anal. Chem.* **2019**, *91*, 7295–7303. [[CrossRef](#)] [[PubMed](#)]
144. Liu, Z.; Liang, Y.; Cao, W.; Gao, W.; Tang, B. Proximity-induced hybridization chain reaction-based photoacoustic imaging system for amplified visualization protein-specific glycosylation in mice. *Anal. Chem.* **2021**, *93*, 8915–8922. [[CrossRef](#)] [[PubMed](#)]
145. Akiba, U.; Anzai, J.I. Recent progress in electrochemical biosensors for glycoproteins. *Sensors* **2016**, *16*, 2045. [[CrossRef](#)] [[PubMed](#)]
146. Shah, A.K.; Hill, M.M.; Shiddiky, M.J.; Trau, M. Electrochemical detection of glycan and protein epitopes of glycoproteins in serum. *Analyst* **2014**, *139*, 5970–5976. [[CrossRef](#)] [[PubMed](#)]
147. Xue, Y.D.; Ding, L.; Lei, J.P.; Ju, H.X. A simple electrochemical lectin-probe for in situ homogeneous cytosensing and facile evaluation of cell surface glycan. *Biosens. Bioelectron.* **2010**, *26*, 169–174. [[CrossRef](#)]
148. Xia, N.; Cheng, C.; Liu, L.; Peng, P.Z.; Liu, C.; Chen, J.X. Electrochemical glycoprotein aptasensors based on the in-situ aggregation of silver nanoparticles induced by 4-mercaptophenylboronic acid. *Microchim. Acta* **2017**, *184*, 4393–4400. [[CrossRef](#)]
149. Chang, Y.; Liu, G.; Li, S.; Liu, L.; Song, Q.J. Biorecognition element-free electrochemical detection of recombinant glycoproteins using metal-organic frameworks as signal tags. *Anal. Chim. Acta* **2023**, *1273*, 341540. [[CrossRef](#)]
150. Chen, X.J.; Wang, Y.Z.; Zhang, Y.Y.; Chen, Z.H.; Liu, Y.; Li, Z.L.; Li, J.H. Sensitive electrochemical aptamer biosensor for dynamic cell surface N-glycan evaluation featuring multivalent recognition and signal amplification on a dendrimer-graphene electrode interface. *Anal. Chem.* **2014**, *86*, 4278–4286. [[CrossRef](#)]
151. Liu, J.X.; Bao, N.; Luo, X.; Ding, S.N. Nonenzymatic amperometric aptamer cytosensor for ultrasensitive detection of circulating tumor cells and dynamic evaluation of cell surface N-glycan expression. *ACS Omega* **2018**, *3*, 8595–8604. [[CrossRef](#)]
152. Yang, H.Y.; Li, Z.J.; Wei, X.M.; Huang, R.; Qi, H.L.; Gao, Q.; Li, C.Z.; Zhang, C.X. Detection and discrimination of alpha-fetoprotein with a label-free electrochemical impedance spectroscopy biosensor array based on lectin functionalized carbon nanotubes. *Talanta* **2013**, *111*, 62–68. [[CrossRef](#)] [[PubMed](#)]
153. Zhang, X.A.; Teng, Y.Q.; Fu, Y.; Zhang, S.P.; Wang, T.; Wang, C.G.; Jin, L.; Zhang, W. Lectin-based electrochemical biosensor constructed by functionalized carbon nanotubes for the competitive assay of glycan expression on living cancer cells. *Chem. Sci.* **2011**, *2*, 2353–2360. [[CrossRef](#)]
154. Rivnay, J.; Inal, S.; Salleo, A.; Owens, R.M.; Berggren, M.; Malliaras, G.G. Organic electrochemical transistors. *Nat. Rev. Mater.* **2018**, *3*, 17086. [[CrossRef](#)]
155. Chen, L.Z.; Wang, N.X.; Wu, J.; Yan, F.; Ju, H.X. Organic electrochemical transistor for sensing of sialic acid in serum samples. *Anal. Chim. Acta* **2020**, *1128*, 231–237. [[CrossRef](#)] [[PubMed](#)]
156. Liao, C.; Mak, C.; Zhang, M.; Chan, H.L.; Yan, F. Flexible organic electrochemical transistors for highly selective enzyme biosensors and used for saliva testing. *Adv. Mater.* **2015**, *27*, 676–681. [[CrossRef](#)]

157. Chen, L.Z.; Fu, Y.; Wang, N.X.; Yang, A.N.; Li, Y.Z.; Wu, J.; Ju, H.; Yan, F. Organic electrochemical transistors for the detection of cell surface glycans. *ACS Appl. Mater. Interfaces* **2018**, *10*, 18470–18477. [[CrossRef](#)]
158. Chen, L.Z.; Wu, J.; Yan, F.; Ju, H.X. Monose-modified organic electrochemical transistors for cell surface glycan analysis via competitive recognition to enzyme-labeled lectin. *Microchim. Acta* **2021**, *188*, 252. [[CrossRef](#)]
159. Chen, L.Z.; Wu, J.; Yan, F.; Ju, H.X. A facile strategy for quantitative sensing of glycans on cell surface using organic electrochemical transistors. *Biosens. Bioelectron.* **2021**, *175*, 112878. [[CrossRef](#)]
160. Zhang, J.J.; Cheng, F.F.; Zheng, T.T.; Zhu, J.J. Versatile aptasensor for electrochemical quantification of cell surface glycan and naked-eye tracking glycolytic inhibition in living cells. *Biosens. Bioelectron.* **2017**, *89*, 937–945. [[CrossRef](#)]
161. Qian, R.C.; Ding, L.; Bao, L.; He, S.J.; Ju, H.X. In situ electrochemical assay of cell surface sialic acids featuring highly efficient chemoselective recognition and a dual-functionalized nanohorn probe. *Chem. Commun.* **2012**, *48*, 3848–3850. [[CrossRef](#)]
162. Hu, Q.; Wan, J.W.; Liang, Z.W.; Li, S.Q.; Feng, W.X.; Liang, Y.Y.; Luo, Y.L.; Cao, X.J.; Ma, Y.M.; Han, D.X.; et al. Dually amplified electrochemical aptasensor for endotoxin detection via target-assisted electrochemically mediated ATRP. *Anal. Chem.* **2023**, *95*, 5463–5469. [[CrossRef](#)] [[PubMed](#)]
163. Zhang, X.A.; Lu, W.J.; Shen, J.Z.; Jiang, Y.X.; Han, E.; Dong, X.Y.; Huang, J.L. Carbohydrate derivative-functionalized biosensing toward highly sensitive electrochemical detection of cell surface glycan expression as cancer biomarker. *Biosens. Bioelectron.* **2015**, *74*, 291–298. [[CrossRef](#)] [[PubMed](#)]
164. Ding, L.; Ji, Q.J.; Qian, R.C.; Cheng, W.; Ju, H.X. Lectin-based nanoprobe functionalized with enzyme for highly sensitive electrochemical monitoring of dynamic carbohydrate expression on living cells. *Anal. Chem.* **2010**, *82*, 1292–1298. [[CrossRef](#)] [[PubMed](#)]
165. Han, E.; Ding, L.; Jin, S.; Ju, H.X. Electrochemiluminescent biosensing of carbohydrate-functionalized CdS nanocomposites for in situ label-free analysis of cell surface carbohydrate. *Biosens. Bioelectron.* **2011**, *26*, 2500–2505. [[CrossRef](#)] [[PubMed](#)]
166. Han, E.; Ding, L.; Lian, H.; Ju, H.X. Cytosensing and dynamic monitoring of cell surface carbohydrate expression by electrochemiluminescence of quantum dots. *Chem. Commun.* **2010**, *46*, 5446–5448. [[CrossRef](#)] [[PubMed](#)]
167. Zhou, H.; Yang, Y.Y.; Li, C.X.; Yu, B.; Zhang, S.S. Enhanced iridium complex electrochemiluminescence cytosensing and dynamic evaluation of cell-surface carbohydrate expression. *Chem. Eur. J.* **2014**, *20*, 14736–14743. [[CrossRef](#)] [[PubMed](#)]
168. Wang, Y.Z.; Chen, Z.H.; Liu, Y.; Li, J.H. A functional glycoprotein competitive recognition and signal amplification strategy for carbohydrate-protein interaction profiling and cell surface carbohydrate expression evaluation. *Nanoscale* **2013**, *5*, 7349–7355. [[CrossRef](#)] [[PubMed](#)]
169. Chen, Z.H.; Liu, Y.; Wang, Y.Z.; Zhao, X.; Li, J.H. Dynamic evaluation of cell surface N-glycan expression via an electrogenerated chemiluminescence biosensor based on concanavalin A-integrating gold-nanoparticle-modified Ru(bpy)₃²⁺-doped silica nanoprobe. *Anal. Chem.* **2013**, *85*, 4431–4438. [[CrossRef](#)]
170. Chen, X.J.; He, Y.; Zhang, Y.Y.; Liu, M.L.; Liu, Y.; Li, J.H. Ultrasensitive detection of cancer cells and glycan expression profiling based on a multivalent recognition and alkaline phosphatase-responsive electrogenerated chemiluminescence biosensor. *Nanoscale* **2014**, *6*, 11196–11203. [[CrossRef](#)]
171. Ma, W.; Xu, S.; Liu, H.W.; Bai, Y. Mass spectrometry methods for in situ analysis of clinical biomolecules. *Small Methods* **2020**, *4*, 1900407. [[CrossRef](#)]
172. Ma, W.; Xu, S.T.; Nie, H.G.; Hu, B.Y.; Bai, Y.; Liu, H.W. Bifunctional cleavable probes for in situ multiplexed glycan detection and imaging using mass spectrometry. *Chem. Sci.* **2019**, *10*, 2320–2325. [[CrossRef](#)] [[PubMed](#)]
173. Dressman, J.W.; McDowell, C.T.; Lu, X.; Angel, P.M.; Drake, R.R.; Mehta, A.S. Development of an antibody-based platform for the analysis of immune cell-specific N-linked glycosylation. *Anal. Chem.* **2023**, *95*, 10289–10297. [[CrossRef](#)] [[PubMed](#)]
174. Powers, T.W.; Jones, E.E.; Betesh, L.R.; Romano, P.R.; Gao, P.; Copland, J.A.; Mehta, A.S.; Drake, R.R. Matrix assisted laser desorption ionization imaging mass spectrometry workflow for spatial profiling analysis of N-linked glycan expression in tissues. *Anal. Chem.* **2013**, *85*, 9799–9806. [[CrossRef](#)]
175. Dai, C.; Cazares, L.H.; Wang, L.; Chu, Y.; Wang, S.L.; Troyer, D.A.; Semmes, O.J.; Drake, R.R.; Wang, B. Using boronolactin in MALDI-MS imaging for the histological analysis of cancer tissue expressing the sialyl Lewis X antigen. *Chem. Commun.* **2011**, *47*, 10338–10340. [[CrossRef](#)] [[PubMed](#)]
176. He, Z.Y.; Chen, Q.S.; Chen, F.M.; Zhang, J.; Li, H.F.; Lin, J.M. DNA-mediated cell surface engineering for multiplexed glycan profiling using MALDI-TOF mass spectrometry. *Chem. Sci.* **2016**, *7*, 5448–5452. [[CrossRef](#)]
177. Han, J.; Huang, X.; Liu, H.H.; Wang, J.Y.; Xiong, C.Q.; Nie, Z.X. Laser cleavable probes for in situ multiplexed glycan detection by single cell mass spectrometry. *Chem. Sci.* **2019**, *10*, 10958–10962. [[CrossRef](#)]
178. Sun, J.; Liu, H.; Zhan, L.; Xiong, C.; Huang, X.; Xue, J.; Nie, Z.X. Laser cleavable probes-based cell surface engineering for in situ sialoglycoconjugates profiling by laser desorption/ionization mass spectrometry. *Anal. Chem.* **2018**, *90*, 6397–6402. [[CrossRef](#)]
179. Sun, B.; Xu, F.F.; Zhang, Y.Y.; Hu, Y.C.; Chen, Y. Dual-probe approach for mass spectrometric quantification of MUC1-specific terminal Gal/GalNAc in situ. *Anal. Chem.* **2020**, *92*, 8340–8349. [[CrossRef](#)]

Disclaimer/Publisher's Note: The statements, opinions and data contained in all publications are solely those of the individual author(s) and contributor(s) and not of MDPI and/or the editor(s). MDPI and/or the editor(s) disclaim responsibility for any injury to people or property resulting from any ideas, methods, instructions or products referred to in the content.